NASA/CR-2020-5001870

Development of a Weather-Robust Ground-Based System for Sonic Boom Measurements

Kent L. Gee, Daniel J. Novakovich, Logan T. Mathews,
Mark C. Anderson, and Reese D. Rasband
Brigham Young University, Provo, Utah

Prepared for:
National Aeronautics and Space Administration
Langley Research Center, Hampton, VA

Contract 80LARC17C0004, Activity 201110
Alexandra Loubeau, Technical Monitor

July 2020

NASA STI Program ... in Profile

Since its founding, NASA has been dedicated to the advancement of aeronautics and space science. The NASA scientific and technical information (STI) program plays a key part in helping NASA maintain this important role.

The NASA STI program operates under the auspices of the Agency Chief Information Officer. It collects, organizes, provides for archiving, and disseminates NASA's STI. The NASA STI program provides access to the NTRS Registered and its public interface, the NASA Technical Reports Server, thus providing one of the largest collections of aeronautical and space science STI in the world. Results are published in both non-NASA channels and by NASA in the NASA STI Report Series, which includes the following report types:

- TECHNICAL PUBLICATION. Reports of completed research or a major significant phase of research that present the results of NASA Programs and include extensive data or theoretical analysis. Includes compilations of significant scientific and technical data and information deemed to be of continuing reference value. NASA counterpart of peer-reviewed formal professional papers but has less stringent limitations on manuscript length and extent of graphic presentations.

- TECHNICAL MEMORANDUM. Scientific and technical findings that are preliminary or of specialized interest, e.g., quick release reports, working papers, and bibliographies that contain minimal annotation. Does not contain extensive analysis.

- CONTRACTOR REPORT. Scientific and technical findings by NASA-sponsored contractors and grantees.

- CONFERENCE PUBLICATION. Collected papers from scientific and technical conferences, symposia, seminars, or other meetings sponsored or co-sponsored by NASA.

- SPECIAL PUBLICATION. Scientific, technical, or historical information from NASA programs, projects, and missions, often concerned with subjects having substantial public interest.

- TECHNICAL TRANSLATION. English-language translations of foreign scientific and technical material pertinent to NASA's mission.

Specialized services also include organizing and publishing research results, distributing specialized research announcements and feeds, providing information desk and personal search support, and enabling data exchange services.

For more information about the NASA STI program, see the following:

- Access the NASA STI program home page at http://www.sti.nasa.gov

- E-mail your question to help@sti.nasa.gov

- Phone the NASA STI Information Desk at 757-864-9658

- Write to:
  NASA STI Information Desk
  Mail Stop 148
  NASA Langley Research Center
  Hampton, VA 23681-2199

NASA/CR-2020-5001870

Development of a Weather-Robust Ground-Based System for Sonic Boom Measurements

Kent L. Gee, Daniel J. Novakovich, Logan T. Mathews,
Mark C. Anderson, and Reese D. Rasband
Brigham Young University, Provo, Utah

National Aeronautics and
Space Administration

Langley Research Center
Hampton, VA

July 2020

Development of a Weather-Robust Ground-Based System for Sonic Boom Measurements

Kent L. Gee, Principal Investigator
Professor of Physics
Brigham Young University

Contributors: Daniel J. Novakovich, Logan T. Mathews, Mark C. Anderson, and Reese D. Rasband

Draft Submitted: 13 March 2020

Revision Submitted: 31 March 2020

Project Number: NIA C18-201110-BYU

Table of Contents

Acknowledgments

This program was supported by the National Institute of Aerospace, with Susan Sorlie as contract monitor. Dr. Alexandra Loubeau of NASA Langley Research Center was the program manager and we thank her for her careful oversight and guidance. Jacob Klos, Joel Lonzaga, William Doebler, and Edward Haering provided helpful feedback during report preparation. We express appreciation to all those NASA and other personnel who made sonic boom field testing possible. We also thank colleagues and collaborators who contributed to the findings in the report: Per Rasmussen of GRAS Sound and Vibration, Thomas Gabrielson of Penn State, and to colleagues at Blue Ridge Research and Consulting, LLC who contributed to the initial hardware design and whose usage of it for various outdoor sound measurement projects has provided additional feedback. Finally, we express appreciation to dedicated Brigham Young University students who participated in sonic boom testing: Kevin Leete, Taylor Kimball, Mylan Cook, Jacob Ward, and Aaron Vaughn.

1. Executive Summary: Overview

This report describes Brigham Young University's (BYU) development and testing of a weather-robust, ground-based system for sonic boom measurements, carried out in support of NASA's Quiet Supersonic Flight (QSF) initiative. The microphone configuration system, referred to as the Compact Outdoor Unit for Ground-based Acoustical Recordings (COUGAR, for the BYU mascot), was tested at NASA's 2018 Quiet Supersonic Flight (QSF18) campaign and at the subsequent 2019 Carpet Determination in Entirety Measurements (CarpetDIEM) program. Key results are the following:

- COUGAR is suitable for making high-fidelity measurements under adverse weather conditions, including rain, wind, and blowing dust.
- The wind noise rejection of COUGAR is superior to other microphone configurations tested and a refined system, the COUGARxt, improves upon the initial development. The addition "xt" refers to an "extra thin" ground plate and an "extra thick" windscreen.
- BYU fielded four stations at QSF18 and eleven stations at CarpetDIEM, and developed a hardened data acquisition system, referred to as the Portable Unit for Measuring Acoustics (PUMA). This is a versatile data acquisition system that is capable of fielding microphone arrays.
- In addition to microphone configurations, different microphone and data acquisition hardware comparisons were made in pursuit of the optimal configuration for broader testing.
- A digital filtering technique has been implemented for low booms to acceptably restore limited low-frequency response for low-noise floor channels, thus providing both accurate waveform shape and metric calculations.
- Several important logistical lessons were learned that contribute to the QSF18 and CarpetDIEM findings, and eventual measurement design for testing with NASA's X-59 Quiet SuperSonic Technology (QueSST) aircraft.

The results of the Research and Development (R&D) program go significantly beyond the original program scope, but the data analyses presented here are mostly limited to understanding performance of microphone systems. However, the data acquired under this program should be further analyzed to improve understanding how both the propagation and measurement environment can contribute to measurement fidelity and variability, which can impact noise exposure estimation during X-59 testing and quiet-boom civil supersonic aircraft certification.

2. Executive Summary: Key Recommendations

Based on laboratory and field testing, we recommend the following data acquisition hardware/microphone combination for portable systems suitable for quiet sonic boom testing:

- **Data acquisition hardware:** we recommend the National Instruments NI 9250 over the NI 9232 or NI 9234 modules because of its low noise floor and because its low-frequency cutoff (-3 dB) is 0.43 Hz.
- **Microphone:** For low-amplitude booms, a prepolarized 12.7 mm (0.5 in) microphone with sensitivity 12-50 mV/Pa should be used. Given the limited spectral bandwidth of low-amplitude boom measurements (<5 kHz), differences between pressure and free-field microphones are not likely to be seen. Regarding the required low-frequency response of the microphone, sonic boom metrics important for human testing heavily penalize (discount) low-frequency energy and so an ordinary 12.7 mm (0.5 in) Type-1 microphone with an ~3 Hz cutoff frequency may be used. For measurements solely for the purpose of perception-weighted metrics calculations, microphone type should be selected based on maximizing dynamic range. However, without lower frequencies (< 1 Hz) represented in the measurement, the pressure waveform will be visibly distorted. This can hamper physical analysis and comparison with modeling efforts. In this case, two alternatives exist: use of an infrasound-type microphone such as the GRAS 47AC or PCB 378A07, both of which have a low-frequency cutoff of ~0.1 Hz but lower sensitivities, or use of digital filtering. Of the two infrasound microphones, we recommend the GRAS 47AC for its larger dynamic range, shorter settling time, and slightly higher sensitivity. Coupled with the NI 9250, waveform distortion for aircraft sonic booms measured by these microphones is minor. However, the second option to employ digital filtering can be used to improve the low-frequency response of regular 12.7 mm (0.5 in) microphones. This capability is demonstrated in this report as part of the QSF18 data analysis as a suitable alternative when the lowest electronic noise is necessary in quiet ambient environments in order to maximize measurement bandwidth.
- **Microphone configuration:** We recommend that the COUGARxt configuration be used for sonic boom testing. This configuration provides a) robustness in inclement weather including wind and significant rain, b) maximum wind noise reduction relative to all other approaches tried, c) high-fidelity acoustic data. The COUGAR configuration is also preferable to other recent sonic boom measurement approaches.

3. Program Objectives

The primary purpose of this cooperative research and development program has been to develop a field-tested microphone system capability for high-fidelity supersonic aircraft sonic boom measurements in adverse weather conditions. The R&D program consisted of the following interrelated objectives:

- Complete laboratory measurements and controlled field experiments in support of system design
- Investigate and implement performance improvements
- Test the microphone systems as part of NASA's sonic boom testing program

This report describes system testing and development, with a particular focus on BYU's measurements made at the NASA QSF18 and CarpetDIEM campaigns.

4. Weather-Robust System Development

4.1. COUGAR and COUGARxt

4.1.1. COUGAR Description

The Compact Outdoor Unit for Ground-based Acoustical Recordings (COUGAR) is a weather-robust microphone system. It was originally developed at BYU as part of a joint project[i] between Blue Ridge Research and Consulting, LLC (BRRC) and BYU in pursuit of improved launch vehicle noise measurements. Under the present R&D program, COUGAR has undergone significant testing for sonic boom measurements under adverse conditions. COUGAR consists of four elements: a convex plate, a tripod

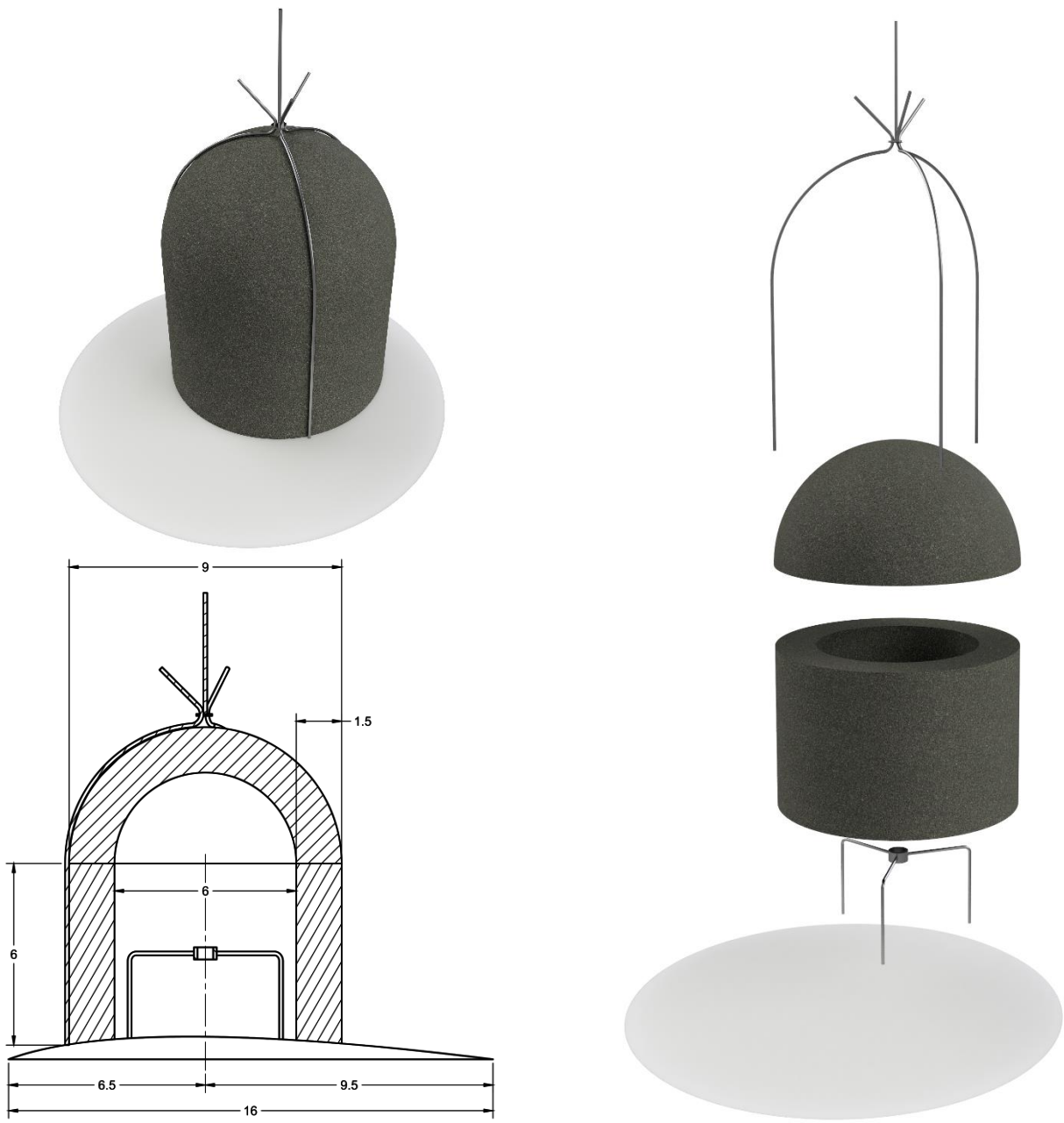

Figure 4-1. COUGAR (top left), with its individual parts (right) and a side cutaway view (bottom left).

inverted microphone mount, a two-piece polyurethane foam windscreen, and a collapsible bird spike assembly. COUGAR is shown in Figure 4-2. COUGAR positions an inverted 12.7 mm (0.5 in) microphone in the welded holder, above the apex of a convex, 0.406 m (16 in) plate machined from UHMW polyethylene. The apex of the plate is 20 mm (0.8 in) thick and is off center by 38 mm (1.5 in) to reduce symmetry and possibly reduce high-frequency interference effects by acoustic scattering off the edge of the plate. The microphone height is adjustable with a set screw on the holder but is usually set with the microphone diaphragm height equal to one-half its diameter, in keeping with long-standing tradition[ii,iii] in the acoustics test community regarding inverted microphone setups. The microphone assembly is surrounded by a 40 mm (1.5 in) thick reticulated polyurethane foam windscreen, with 18 pores per inch (ppi). The foam thickness and density came from discussions with Per Rasmussen, President of GRAS Sound and Vibration and leading expert in the field of laboratory-quality microphone systems. A hydrophobic coating was investigated but did not improve water resistance. The reticulated foam and the windscreen shape provide significant water wicking, preventing precipitation from reaching the microphone. The bird spike assembly fits over the top of the windscreen, preventing fowl from landing on top of the setup, and its legs fit into holes in the plate, securely anchoring the windscreen to the plate.

The plate convexity, microphone positioning slightly above the plate, windscreen shape, and bird spikes that tend to channel water along the outside of the screen, are all intended to prevent precipitation from reaching the microphone while still yielding high-fidelity recordings. However, in the case of extreme rainfall, a thin rain cap made of tent nylon and Velcro hooks may be fitted into the inside of the top of the windscreen dome. This further prohibits precipitation from reaching the microphone through the top of the dome.

4.1.2. Development of COUGARxt

While COUGAR provides excellent wind noise rejection in a weather-robust package, some improvements have been completed after laboratory measurements and analysis of QSF18 data. This new iteration, which modifies the plate material and thickness along with the windscreen thickness (while keeping the

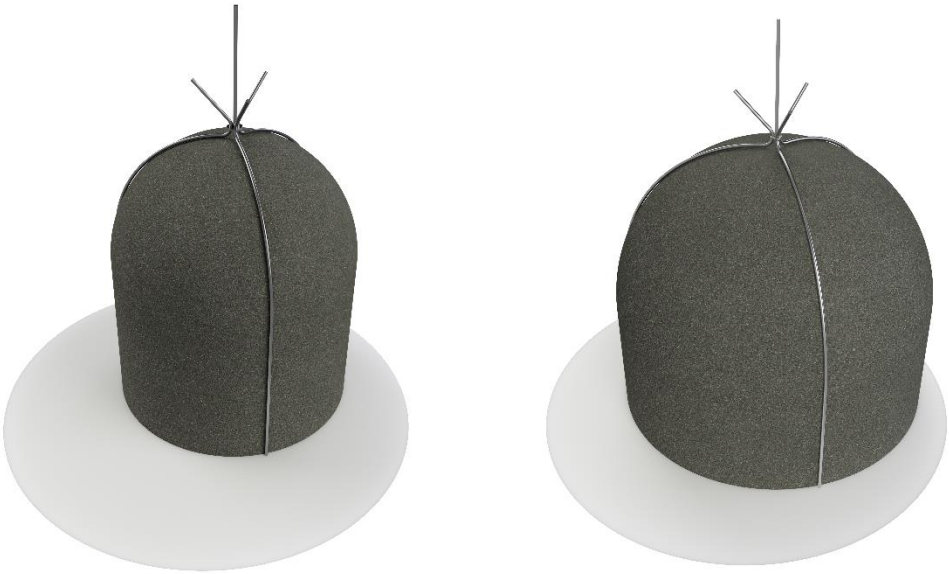

Figure 4-3. COUGAR (left) and COUGARxt (right). While maintaining the same overall height, COUGARxt offers a windscreen twice as thick as COUGAR.

same overall height for transportability) is referred to as COUGARxt (where the “xt” stands for the “extra thick” windscreen and the “extra thin” plate). COUGARxt features a windscreen thickness of 76 mm (3.0 in) and features a thinner ground plate machined out of Delrin®, a stiffer POM polymer, with a less pronounced bulge at the apex. The use of Delrin® allows for the thinner plate while preventing plate warping. COUGAR and COUGARxt comparisons were part of the CarpetDIEM tests, laboratory, and other field measurements.

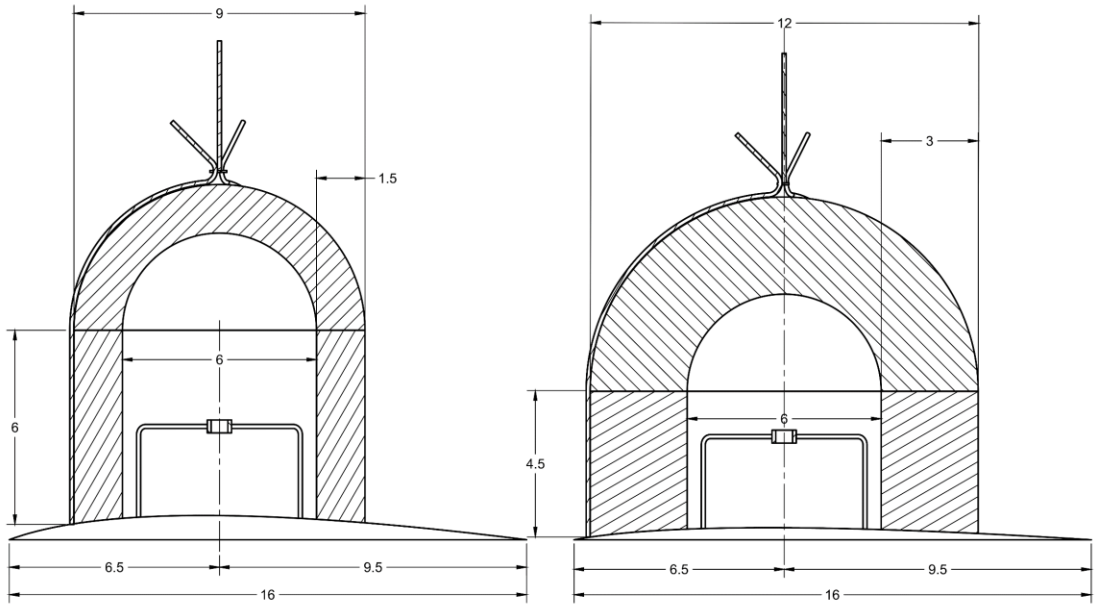

Figure 4-4. Schematic comparing COUGAR (left) and COUGARxt (right). Notice the thinner profile ground plate and thicker windscreen of COUGARxt while not exceeding the height of COUGAR. Dimensions are given in inches.

4.2. Data Acquisition System Description

4.2.1. PUMA System

Although the primary emphasis of this R&D program was not to develop full data acquisition (DAQ) systems, optimizing the microphone configuration alone does not ensure recording fidelity. High-fidelity sonic boom measurements under adverse weather conditions require that all hardware be considered. Under this program, and aided by preliminary development for launch vehicle measurements, the Portable Unit for Measuring Acoustics (PUMA) was developed to provide a rapidly-deployable, compact, and weather-robust data acquisition system for sonic boom measurements. In addition to high-fidelity acoustic data acquisition, PUMA allows for local meteorological data collection and GPS-synchronized time data using the IRIG-B protocol.

4.2.1.1. Hardware

The PUMA system is based upon a compact and versatile architecture. At its core, it features a PC-based high-fidelity data acquisition system with supporting elements. PUMA consists of six main elements:

1. A ruggedized, weather-robust and insulated case with cable and ventilation ports, featuring USB-powered 30 mm (1.2 in) axial cooling fans in a push-pull configuration for active ventilation.

2. A rechargeable and long-lasting 185 Wh/50,000 mAh power supply, capable of providing both 12V and 20V power to the data acquisition and ventilation systems, as well as 5V USB power at both 1.2 and 2.4A. The Maxoak™ supply chosen permits pass-through charging, which allows for concurrent use of an 18 V, 50 or 100 W solar charger.
3. A Windows® tablet PC with the BYU/BRRC Acoustic Field Recorder (AFR) software.
4. A National Instruments™ CompactDAQ chassis and module(s) with USB connectivity. For this program, both the single-slot USB-9171 and the four-slot USB-9174 chassis were used. Modules tested, each with their pros and cons, were the NI 9234, NI 9232, and the NI 9250.
5. A Kestrel® 4X00-series weather meter, connecting to the data acquisition computer/software via Bluetooth.

Figure 4-5 shows PUMA components (except for the waterproof solar panel). Different PUMA configurations were used for QSF18 and CarpetDIEM, and this is described in the measurement and analysis summaries. Figure 4-6 shows a partially assembled PUMA.

Figure 4-5. PUMA components clockwise from top left: Kestrel weather meter, ruggedized case with ventilation and cable ports, GPS time clock and antenna, Surface Pro Windows tablet PC, rechargeable 50,000 mAh power supply, National Instruments compact DAQ chassis populated with modules. The 50-100 W solar panel used to charge the power supply is not shown.

Figure 4-6. PUMA system complete with all components. In field operation, all components can fit inside with the lid closed and secured.

4.2.1.2. Software

PUMA uses a Windows® tablet PC (at present, Surface Pro® 4, 5, 6 and Surface Go®) with BYU/BRRC-developed software called Acoustic Field Recorder (AFR) to make high-fidelity measurements. AFR is a complete software solution for sound and vibration data acquisition in both laboratory and field measurement situations. When combined with the appropriate hardware, professional-grade measurements can be acquired, monitored real-time, and saved for further analysis.

AFR provides the ability to simultaneously configure, calibrate, and record multiple channels, up to hundreds as hardware capabilities permit. Other features are also available to generate output signals, sample and record weather data, and to view and analyze previous recordings.

AFR has manual and autonomous triggering capabilities. Triggering events can be set to occur at a specified time, or when an amplitude threshold is reached on a measurement channel. When a triggering event occurs, the system will automatically record for a specified amount of time (configured by the user) and the resulting data are saved for each measurement channel. AFR can be configured to trigger multiple times for amplitude-based triggering, enabling a PUMA to autonomously capture multiple sonic booms over a long time period, producing individual recordings for each boom.

In addition to recording for a user-specified period, AFR also has the capability to implement a recording buffer. This allows the system to capture a user-specified period of time before the trigger event.

4.3. Laboratory Testing

4.3.1. Objectives

Initial field testing of COUGAR indicated good performance relative to other methods. However, as part of this program, the acoustical performance of COUGAR and COUGARxt have been analyzed in detail. The purpose of this testing was to determine the differences between the configurations in a controlled environment with a known noise source. This allowed us to establish performance relative to a baseline, potentially correct for any systematic discrepancies between the setups in sonic boom measurements, and evaluate potential future design ideas.

4.3.2. Test Apparatus

The configurations were tested in the BYU fully-anechoic (80 Hz – 20 kHz) chamber, which has interior dimensions of 8.8 x 5.8 x 5.8 m (29 x 19.0 x 19.0 ft). Both COUGAR and COUGARxt were tested by varying noise angle of incidence in the elevation and azimuthal directions, thereby creating a three-dimensional representation of their response relative to the known noise source. A photograph of the testing apparatus is shown in Figure 4-7. The testing apparatus consisted of a large arc that extended from five degrees (grazing incidence) to ninety degrees (normal incidence). This arc was attached to a 50 x 100 mm extruded aluminum crossbar for support, and the whole setup was placed on medium-density fiberboard (MDF) boards with a thickness of 19 mm (0.75 in). The boards were used to approximate a hemi-anechoic environment similar to outdoor tests under an open sky. The definitions of the elevation and azimuthal angles are shown in Figure 4-8. White noise was broadcast from a Mackie HR824 mk2 (with a ± 1 dB one-third octave on-axis response between 50 and 20 kHz). To ensure consistency, markings were made on the MDF board to show where the configurations should be placed for each test.

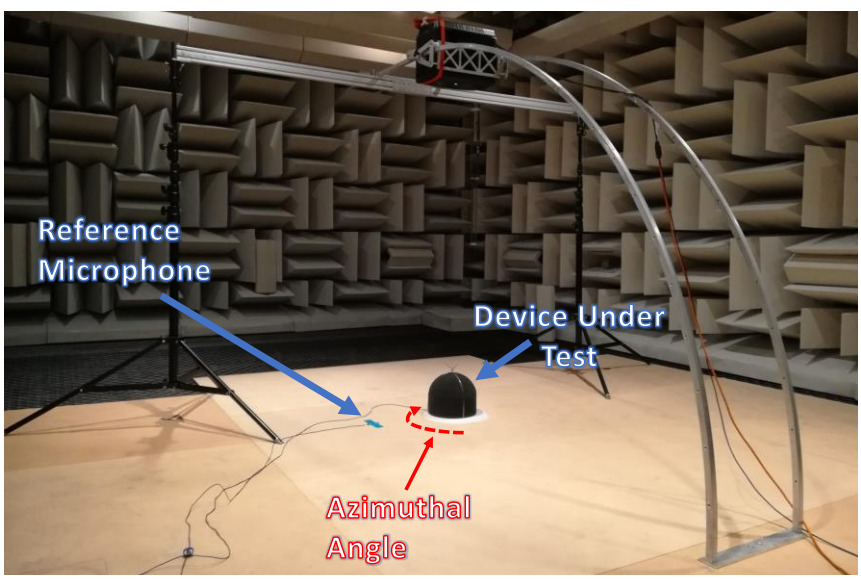

Figure 4-7. The test setup consisted of a round arc with a moveable speaker, attached to a tall crossbar, and oriented with the speaker always pointed directly at the device (configuration) under test. The reference microphone is visible in this picture to the left of the device under test and taped here to the plywood with blue gaffers' tape.

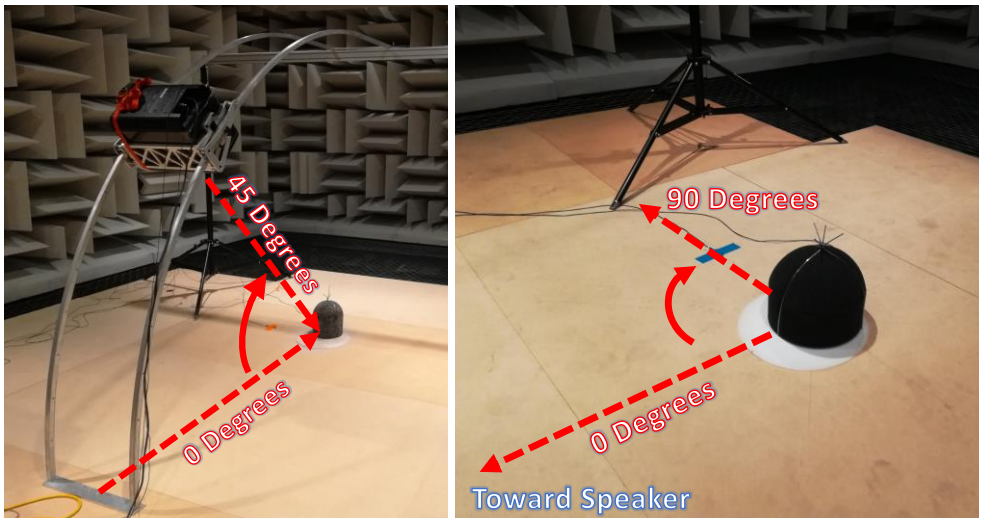

Figure 4-8. Annotated photos showing the angles of incidence used in these measurements. Left: The elevation incidence angle increases as the speaker is moved up the railing. Small angles correspond to near-grazing incidence and large angles correspond to normal incidence relative to the ground. Right: Azimuthal angle, where 0° signifies that the long edge of the plate is oriented toward the sound source.

Overall measurement consistency is within ± 1 dB. For example, a comparison of measurements made one week apart at the reference microphone (see Figure 4-7) is shown in Figure 4-9. At each elevation angle shown, the one-third octave band spectrum (second measurement relative to the first measurement) agrees well, to within 1 dB below 200 Hz and to within 0.5 dB above 200 Hz. The systematic bias of about 0.2 dB is potentially due to loudspeaker heating.

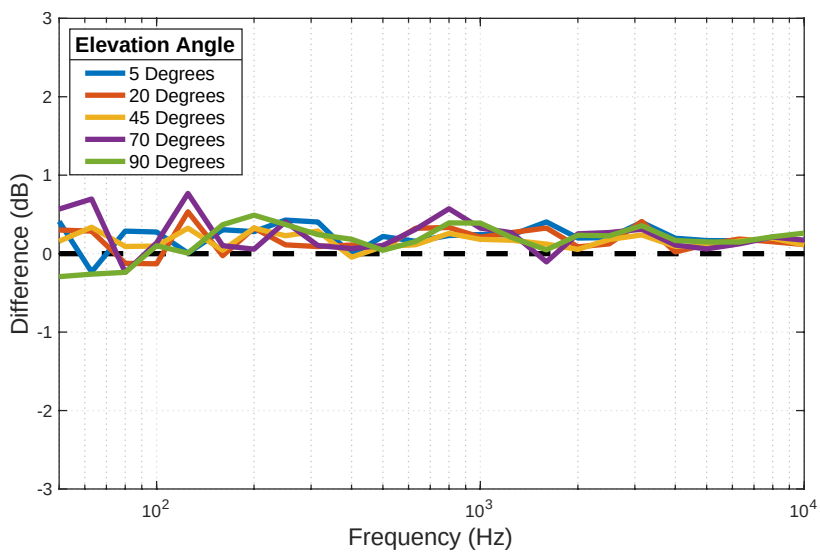

Figure 4-9. Difference between two tests on the regular COUGAR configuration one week apart, measured at the reference microphone.

In addition to testing the different COUGAR/COUGARxt configurations, baseline measurements were made. In this case, "baseline" refers to a measurement made with a 6.35 mm (0.25 in) pressure-field microphone lying flat on the board, with the diaphragm at the center of the setup and oriented orthogonal to the sound propagation path from the speaker. The purpose of the baseline measurement was an

attempt to capture the "ideal" response to each sound field with minimal influence from the microphone installation effects. In this orientation, the pressure-field microphone's response is independent of changes in elevation angle to at least 20 kHz.

4.3.3. Test Design

The COUGAR and COUGARxt tests consisted of a dense test matrix that examined both configurations for a variety of conditions. Elevation incidence angles were tested from 5 – 90° in increments of 5°. Azimuthal angles were tested from 0 – 180° in increments of 45°, with an additional measurement at 270° (to test for symmetry with 90°). Additionally, tests to investigate the effects of the different components of COUGAR were completed, including tests with and without the windscreen to determine windscreen insertion loss. COUGAR was also tested under the environmental extremes of having its windscreen saturated with water and on a separate test saturated with sand. A comparison between data taken using a pressure-field microphone (GRAS 46AO) versus a free-field microphone (GRAS 47AC) is also shown.

4.3.4. Results

Although data were collected at more elevation angles, only 5°, 20°, 45°, 70°, and 90° are shown in the subsequent figures for clarity.

4.3.4.1. Influence of Plate Design

Different potential plate designs for COUGAR were evaluated and minor differences are seen. The relative one-third octave spectra (re: baseline) for the initial COUGAR design in Figure 4-2 is shown in Figure 4-10, whereas Figure 4-11 shows the relative spectra for a thinner plate that measured 9.5 mm (0.38 in) thick at the apex with the same apex offset and Figure 4-12 shows the relative spectra for a COUGAR with the same original thickness but with the apex in the center of the plate. In each case, the plate configurations were tested without the windscreen or bird spikes. A comparison of the three results suggests that the COUGAR plate in Figure 4-10 does cause greater variation in the response between 200 and 900 Hz than the thinner plate in Figure 4-11. In comparing Figure 4-10 and Figure 4-12, however, the location of the plate apex appears to have little impact on the relative one-third octave (OTO) spectrum (at least for this azimuthal angle of 0°). These measurements suggest that a flatter plate is slightly preferable since it does not alter the measurement as much as the thicker plate, which influenced the changes made in COUGARxt. It also suggests that offsetting the apex from the center may not be necessary. Again, in these and all figures that are shown relative to the "baseline," remember that the "baseline" measurement used a 6.35mm (0.25 in) pressure-field microphone lying on its side with the diaphragm orthogonal to the sound field while all microphone configuration measurements used an inverted 12.7 mm (0.5 in) pressure-field microphone.

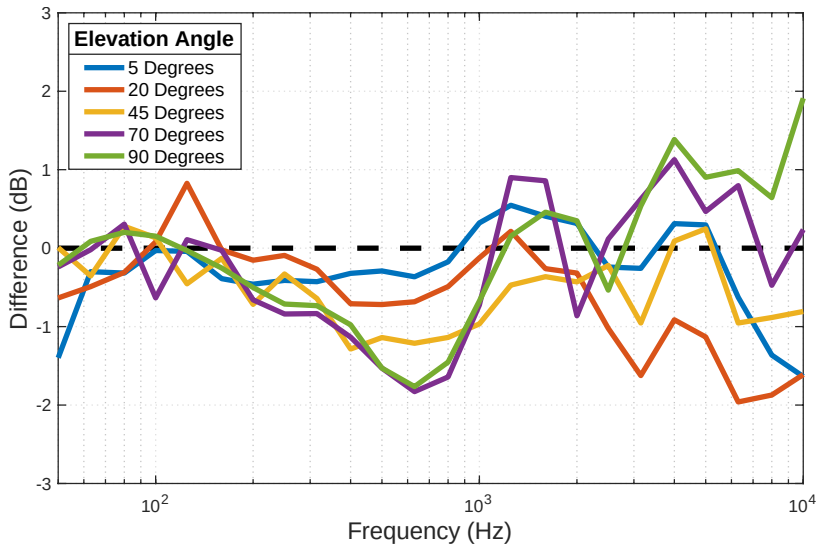

Figure 4-10. One-third octave spectra (re: baseline) from a microphone in a tripod mount and placed 6.35 mm (0.25 in) above the convex COUGAR plate without the windscreen.

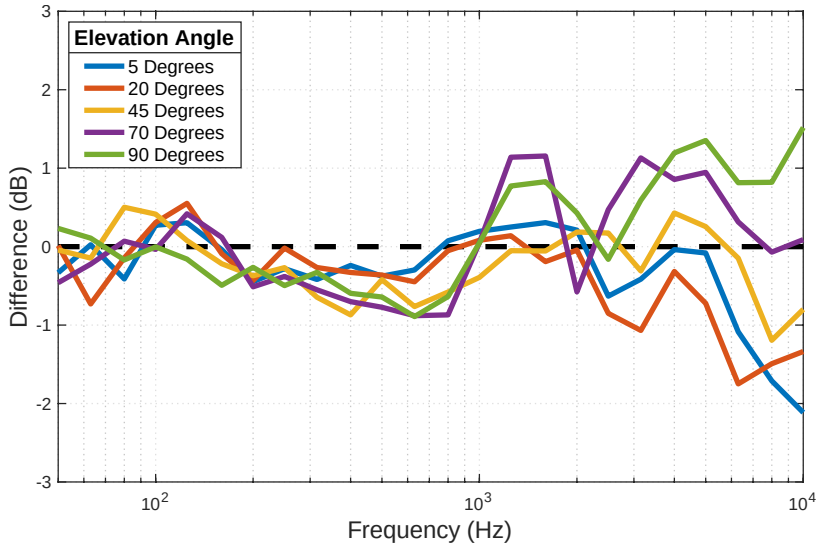

Figure 4-11. One-third octave spectra (re: baseline) of COUGAR without windscreen and with a thinner plate.

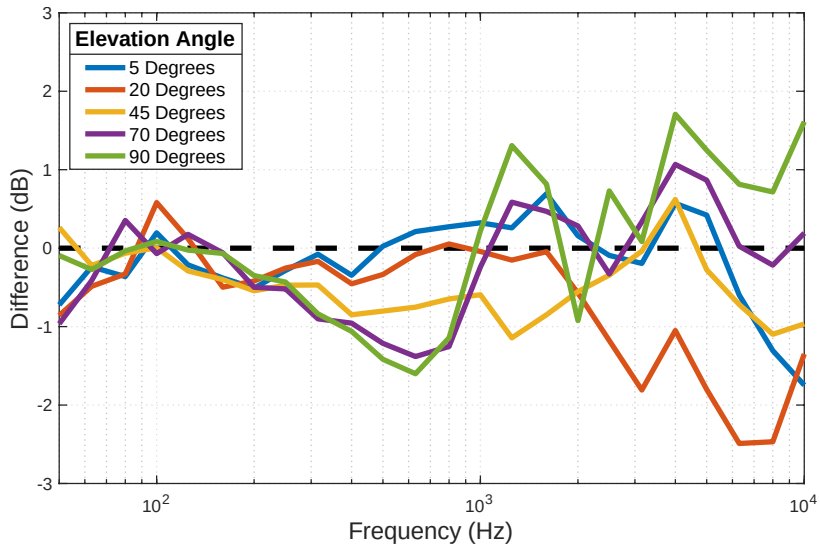

Figure 4-12. One-third octave spectrum (re: baseline) of COUGAR without windscreen and with a plate that has a centered apex.

4.3.4.2. Full COUGAR Performance

Figure 4-13 shows the relative OTO spectrum (re: baseline) for the full COUGAR setup *without* the additional rain cap. Measurements made six months apart on a different COUGAR indicate consistency to within 0.5 dB below 2 kHz and 1 dB above 2 kHz. A comparison of Figure 4-13 with Figure 4-10 suggests that the main variation in COUGAR response as a function of frequency and angle is caused by the plate itself. However, there is a slight downward slope at high frequencies, indicating some absorption by the windscreen. This windscreen absorption is quantified by the difference, in decibels, between Figure 4-10 and Figure 4-13. This difference, which is the negative of the windscreen insertion loss, is shown in Figure 4-14. Excepting 90°, the windscreen losses are nearly independent of angle, with a smooth but slight increase that reaches about 1 dB by 10 kHz. The cause of the high insertion loss behavior at 90° at frequencies above 2 kHz is not currently understood. However, sonic boom elevation angles generally do not approach normal incidence, so this observed behavior at normal incidence is not a cause for concern. Any angle and frequency-dependent effects for COUGAR are less than 2 dB below 1 kHz.

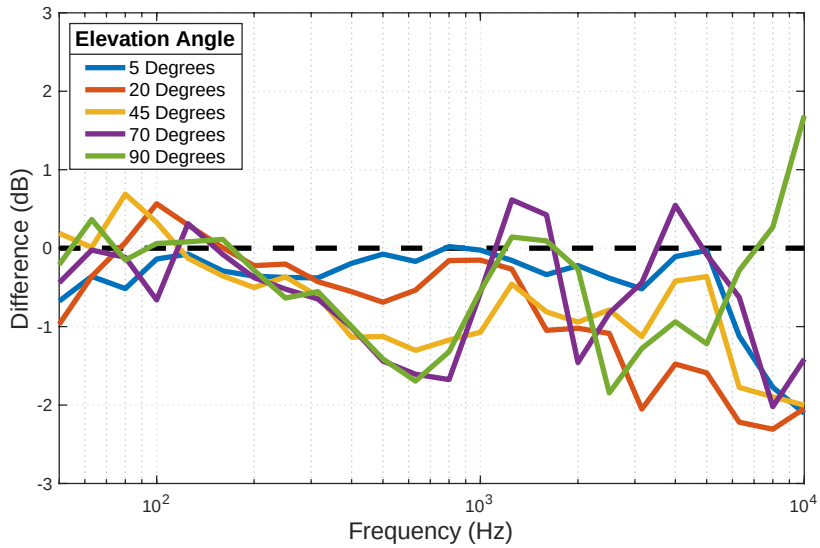

Figure 4-13. One-third octave spectrum (re: baseline) of COUGAR without the additional rain cap.

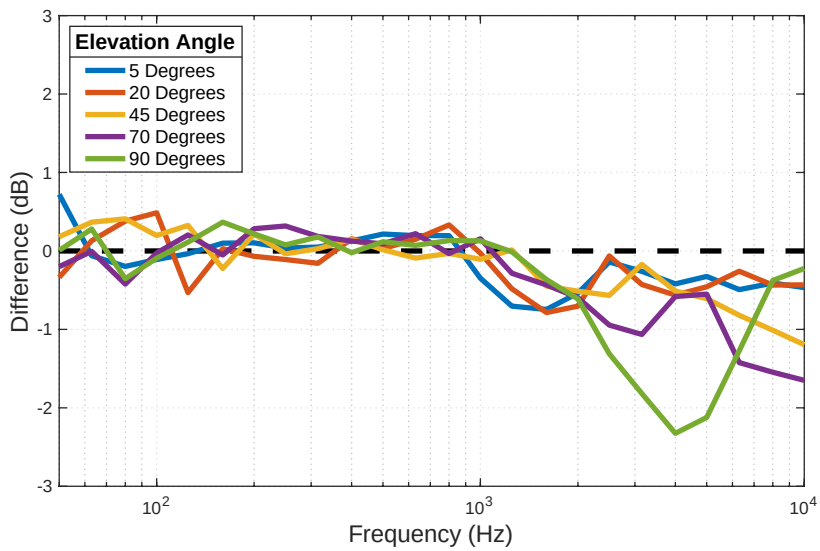

Figure 4-14. Impact of the COUGAR windscreen (without rain cap) on the one-third octave spectrum, for several elevation angles. This graph is the negative of the windscreen insertion loss.

The COUGAR setup was also tested for different plate orientations. These results, for 5° and 45° elevation angles, are shown in Figures 4-15 and 4-16 respectively. Both figures are shown relative to the spectra for 0° azimuth. Overall, there is little dependence on plate azimuthal angle, which one might have supposed based on the little difference in plate apex location shown previously. Thus, it appears relatively unimportant which way a COUGAR is oriented in the field relative to the sound source. This is an informative result to remember during field testing, where the aircraft's flightpath may differ between flights. In these cases, the microphone response is not expected to be affected by different azimuthal arrival angles.

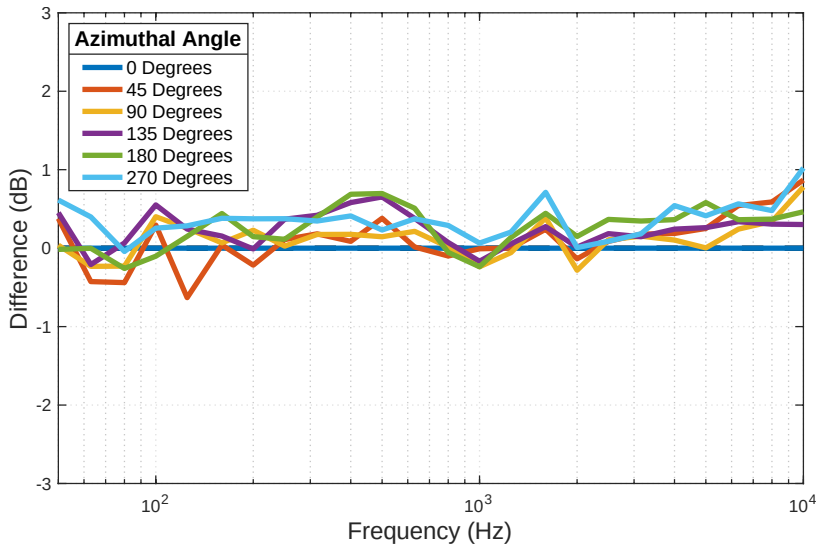

Figure 4-15. One-third octave spectra for COUGAR at 5° elevation angle incidence and different azimuthal angles, relative to 0° azimuth case.

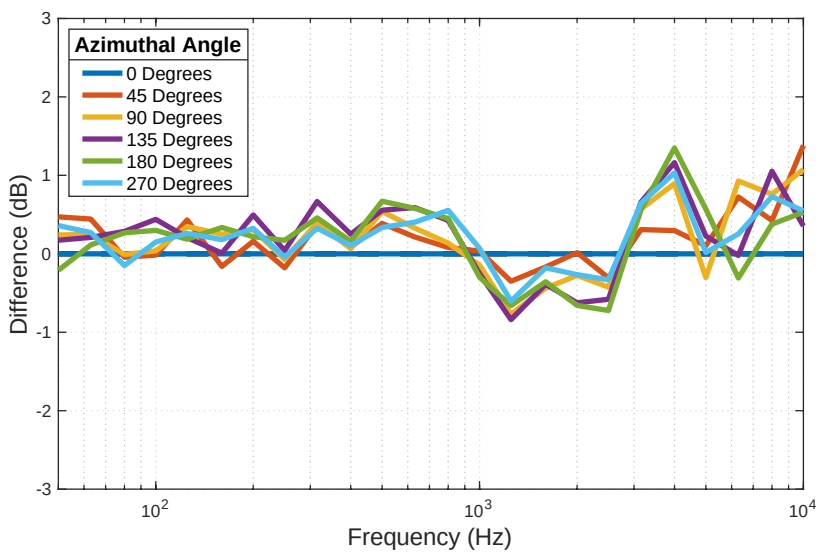

Figure 4-16. One-third octave spectra for COUGAR at 45° elevation angle incidence and different azimuthal angles, relative to 0° azimuth case.

4.3.4.3. Additional Rain Cap Performance

As mentioned previously, a rain cap made of nylon tent material with Velcro hooks can be attached the underside of the COUGAR windscreen dome to ensure that no water comes straight down through the top of the windscreen during a rain event. Relative one-third octave spectra (with rain cap relative to without) are shown in Figure 4-17. For lower angles of incidence (where the sound does not pass through the rain cap), the additional material makes little difference. However, for elevation angles of incidence greater than 45°, the rain cap makes a surprisingly large difference at high frequencies relative to other design considerations. Repeating the rain cap tests on two occasions shows the effects are repeatable to within about 1-2 dB for COUGAR, and similar effects are seen for the COUGARxt design.

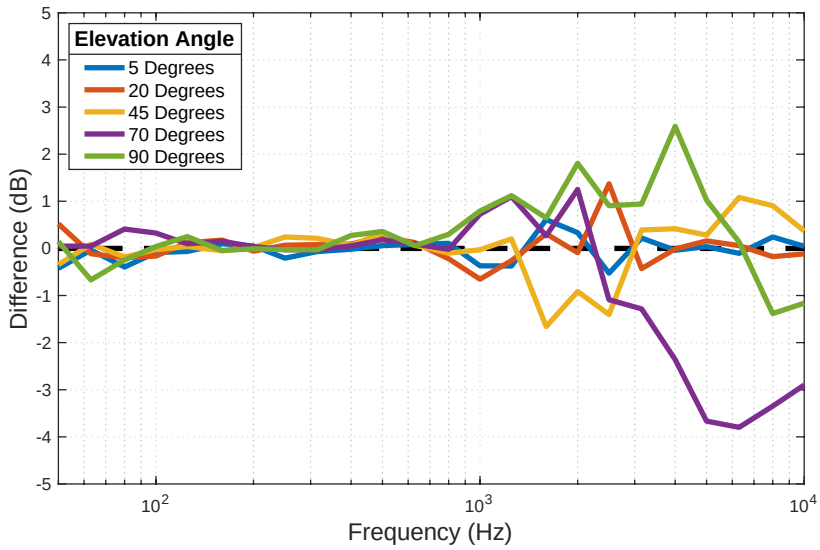

Figure 4-17. One-third octave spectra for the COUGAR configuration with a rain cap relative to a COUGAR configuration without a rain cap.

4.3.4.4. Windscreen Saturation

One of the questions regarding COUGAR is the possible degradation of the acoustic response if the windscreen becomes saturated with water or sand. Figure 4-18 shows the one-third octave spectrum, relative to the dry COUGAR configuration, for several elevation angles as measured after having soaked the windscreen in water. For elevation angles of 45° and below, which roughly corresponds to the range of sonic boom elevation angles expected during flight testing, the variability with frequency is around 1 dB or less across the entire bandwidth. Additionally, the deviation from baseline is no greater than 1 dB for frequencies below 1 kHz for all elevation angles studied here. However, above 1 kHz and for elevation angles greater than 45 degrees, the response changes relative to the dry case by up to 3 to 5 dB. For the sand-infused measurements, play sand was poured through the windscreen until saturated. The measurements were repeated three times, with variable results at high frequencies. One of the three cases is shown in Figure 4-19. In comparing the three different measurements, the variation from the dry configuration is less than 3 dB at all frequencies, but the sand saturation seems to impact the response over a broader range of angles compared to water saturation. It is noted that for the measurements shown it took significant effort to saturate the windscreen because the sand easily slides through the pores. Additionally, the windscreen tended to shed finer particulates, with only aggregates of ~1 mm or larger being retained in the windscreen. This suggests that small amounts of wind-blown sand and soil that may accumulate in the windscreen when deployed in the field probably won't be an issue, or at least won't accumulate in sufficient quantity to affect the acoustic response of the microphone system. In both the cases of water and sand, the measurement artifacts are limited to high frequencies and likely represent an acceptable trade-off to the alternative of not collecting data during inclement weather or having to travel to a remote location to wring or clean out the windscreen before resuming data collection.

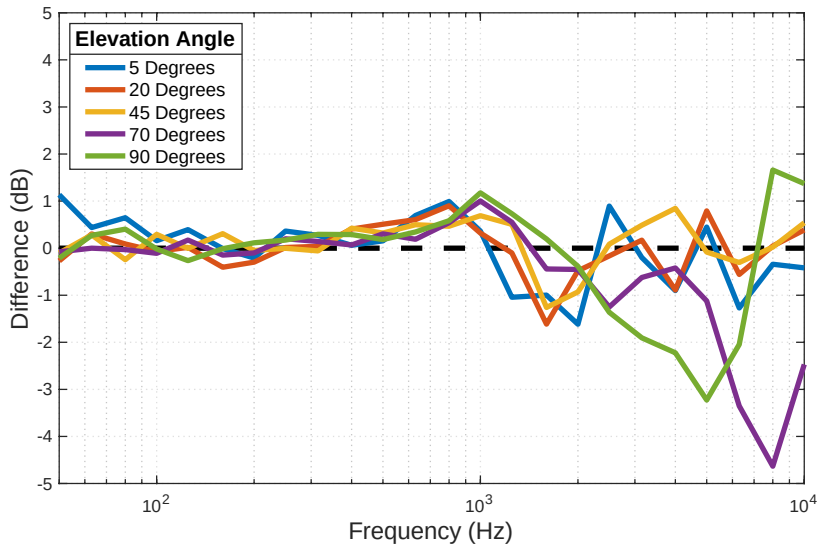

Figure 4-18. One-third octave COUGAR spectrum with the windscreen saturated with water, relative to the dry case. The rain cap was present for all measurements.

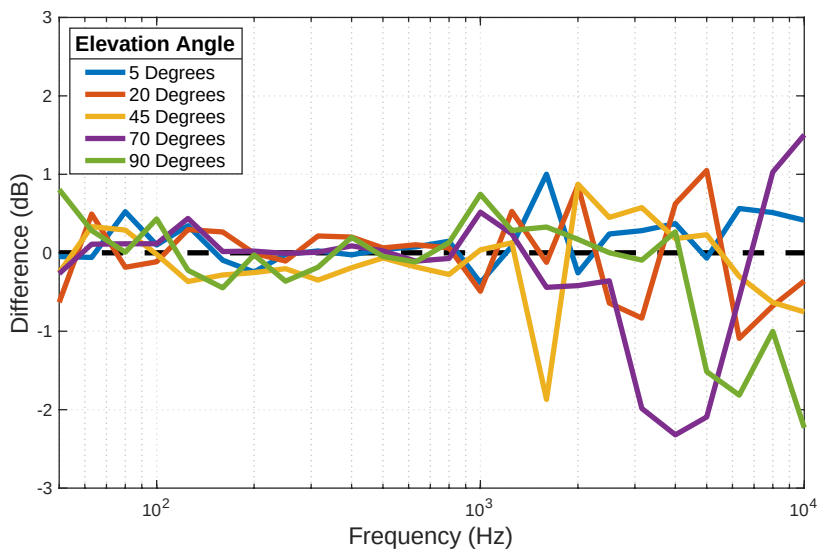

Figure 4-19. One-third octave COUGAR spectrum with the windscreen saturated with sand, relative to the dry case. The rain cap was present for all measurements.

4.3.4.5. Free-field vs. pressure-field microphone

A test of a COUGAR using a free-field microphone versus a pressure-field microphone was completed to see how COUGAR performs with this different type of microphone. The results are shown in Figure 4-20. The free-field microphone was a GRAS 47AC and rolls off at higher frequencies relative to the pressure-field microphone, which was a GRAS 46AO. For the near-grazing case, the pressure-field microphone's response can be considered flat up to the maximum 10 kHz frequency considered here, whereas the free-field microphone rolls off by approximately 4 dB by 10 kHz. This matches the typical 12.7 mm (0.5 in) free-field vs. pressure-field microphone response in microphone handbooks for grazing incidence in the

absence of the reflecting ground plate. The fact that there is little change in the response with angle of incidence here suggests that a free-field microphone's response could be accounted for by applying the industry correction at grazing incidence. Future analyses will quantitatively investigate this hypothesis.

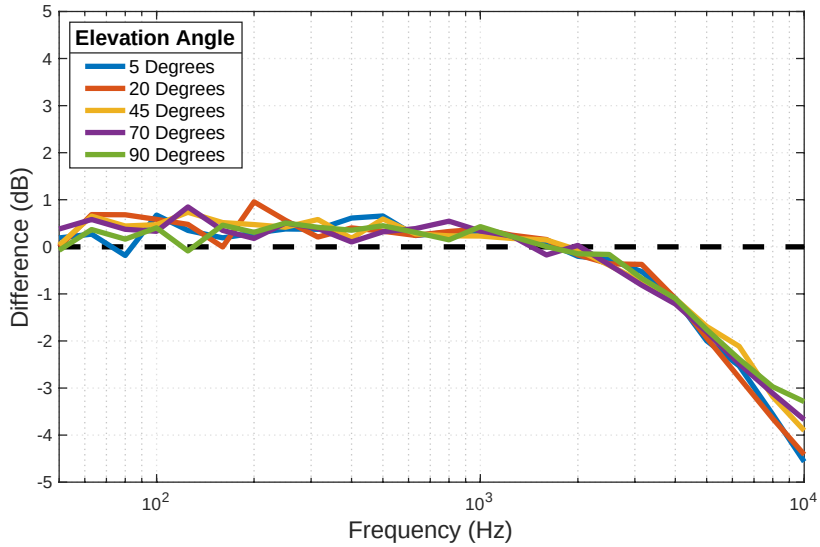

Figure 4-20. COUGAR with a GRAS 46AO relative to COUGAR with a GRAS 47AC. The difference between the two microphones does not have a strong dependence on elevation angle.

4.3.4.6. COUGARxt Performance

A few key results from the full COUGARxt setup (without added rain cap) are shown to demonstrate performance relative to COUGAR. The one-third octave spectra (COUGARxt relative to COUGAR) for different elevation angles are shown in Figure *4-21*. Comparison of Figure *4-21* with Figure 4-13 (COUGAR relative to baseline) indicates that the slight amplification between 200 and 1000 Hz seen in Figure *4-21* actually results in the COUGARxt having a flatter spectrum in this range relative to the baseline. Above 1 kHz, the relative levels for COUGARxt are generally negative, demonstrating slightly greater insertion loss than for COUGAR. This is not surprising, given that the windscreen is twice as thick for COUGARxt. These results suggest the thicker windscreen may be more desirable than the thinner windscreen when measuring sonic boom noise, whose audible frequency content is predominantly below 1 kHz.

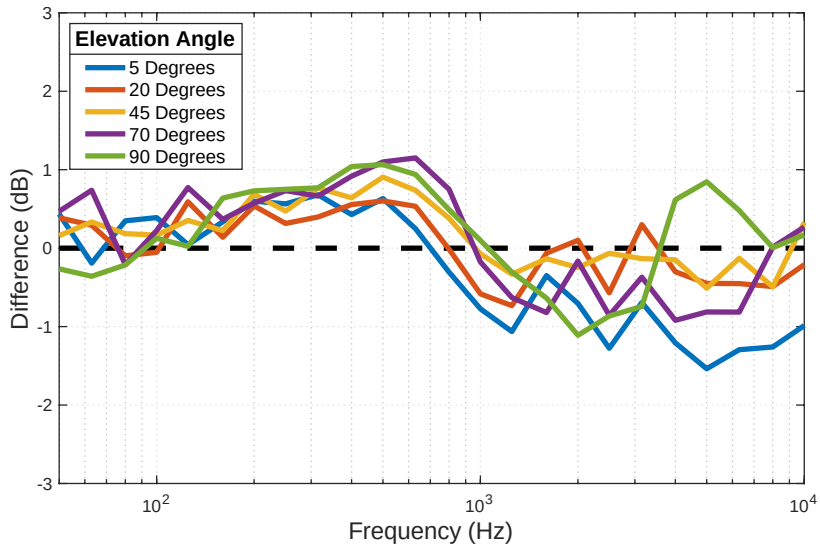

Figure 4-21. One-third octave spectra for the COUGARxt configuration relative to the COUGAR configuration.

Rotation of the COUGARxt configuration for azimuthal angle variation shows similar results to COUGAR, but with slightly less variation at all elevation angles examined. An example is shown in Figure 4-22, with the azimuthally-dependent spectra (relative to the 0° azimuthal angle) for the elevation angle of 45°. Variation, relative to 0°, is less than 1 dB for nearly all frequencies. Comparing this result to COUGAR, which is shown in Figure 4-16, different behavior and slightly less overall variation is observed in the COUGARxt responses. There are two reasons for less overall dependence of plate orientation for COUGARxt relative to COUGAR. First, as described previously, the plate is thinner. Second, the COUGARxt windscreen covers more of the plate, helping to reduce any plate diffraction effects.

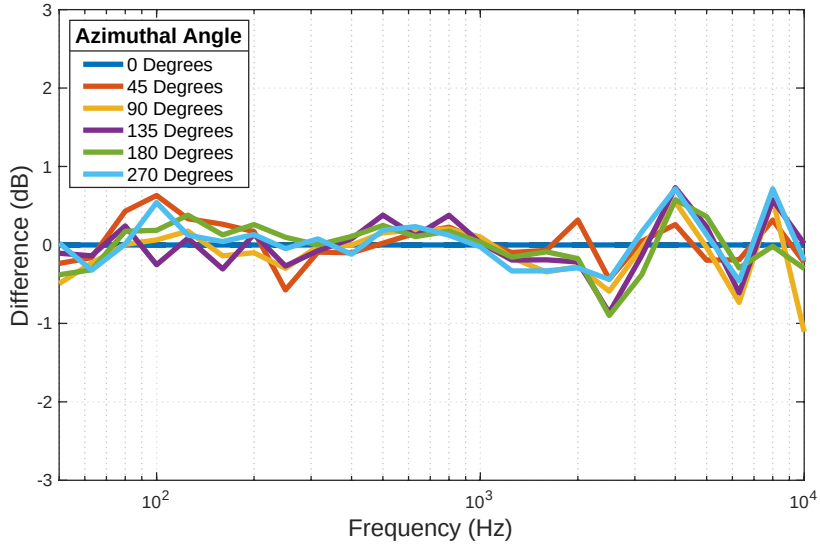

Figure 4-22. One-third octave spectra for COUGARxt at 45° elevation angle incidence and different azimuthal angles, relative to 0° azimuth case.

4.4. Field Testing

4.4.1. Objectives

Covered in this section are field tests beyond QSF18 and CarpetDIEM. These tests were used to examine microphone and data acquisition system performance and otherwise prepare for the sonic boom testing. Three types of tests are described: measurements of a static solid rocket motor, a Space-X Falcon 9 launch and stage-1 reentry sonic boom, and dedicated wind noise rejection testing.

4.4.2. GEM-63 Static Rocket Measurements

Northrop Grumman (formerly Orbital ATK) has a large rocket motor test facility near Promontory, Utah and BYU has frequently used these firings to test instrumentation systems. During the September 2018 firing of the new GEM-63 solid rocket motor (see Figure *4-23*) several different microphone and data acquisition module combinations were tested for low-frequency response and high-frequency noise floor, both of which are important in maximizing measurement bandwidth. The rocket measurements are convenient for this investigation because the rocket motor firing represents a noise source with abundant acoustical energy below 1 Hz and significant averaging times (>90 s).

Figure 4-23. COUGAR testing at a GEM-63 static rocket firing in Promontory, UT, September 2018.

The autospectral density from four channels is shown in Figure 4-24. The first two channels used an NI 9232 module (± 30V, 0.1 Hz cutoff) whereas the last two channels used an NI 9234 module (±5 V, 0.5 Hz cutoff). A 51.2 kHz sampling rate was used. On each of the modules, one of the two channels used a PCB 378A07 free-field microphone, which has a low-frequency cutoff of ~0.13 Hz. The second channel on the NI 9232 module used an ~50 mV/Pa GRAS 40AE microphone whereas the second channel on the NI 9234 module used an ~11 mV/Pa GRAS 40AO pressure microphone. Both of these other microphones have an ~2.5 Hz, 3-dB down cutoff. The autospectral density results reveal that between 3 and 2000 Hz there is

very little difference between the measurements. At the low frequencies, the combination of the NI 9232 module and PCB 378A07 microphone provides the greatest levels, whereas the regular pressure microphone with an NI 9234 module provides the lowest response.

In examining the high-frequency portion of the spectra, improved low-frequency response comes with a price. The PCB 378A07/NI 9232 combination has the highest noise floor, which is caused by the module voltage noise (quantization noise) combined with the relatively low microphone sensitivity. On the other hand, using either the 40AE/NI 9232 or the 40AO/NI 9234 combinations resulted in approximately similar noise floors. We used this measurement to plan for a combination of sensors at each QSF18 station – some to more likely ensure faithful waveform shape reproduction by having an adequate low-frequency response, and others with the lowest possible noise floor. This latter combination turned out to be the 40AE with a newly purchased NI 9250 module that lowers the noise floor by an additional 10 dB. That module had not yet been purchased at the time of the rocket firing event shown in Figure 4-24.

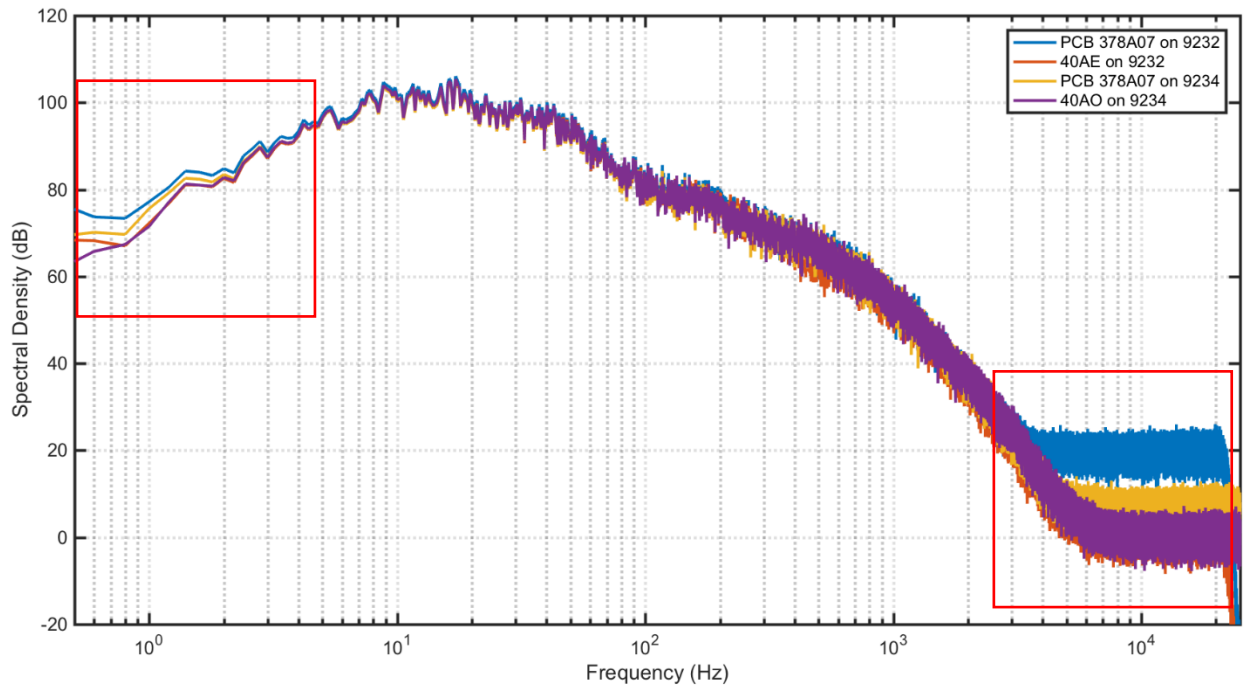

Figure 4-24. Autospectral density at four channels from the GEM-63 measurements, all with COUGAR configurations.

A GEM-63 firing in October 2019 was used to confirm the relative acoustical performance of COUGARxt vs. COUGAR performance. The spectral comparison of COUGARxt (re: COUGAR) is shown in Figure 4-25. The differences are between $\pm$1.5 dB at all frequencies, with attenuation at high frequencies likely due in part to the greater absorption of the COUGARxt windscreen (also seen in the laboratory testing documented in Figure *4-21*). Despite the minor differences, the results in Figure 4-25 show the acoustical similarity between the two outdoor microphone configuration systems.

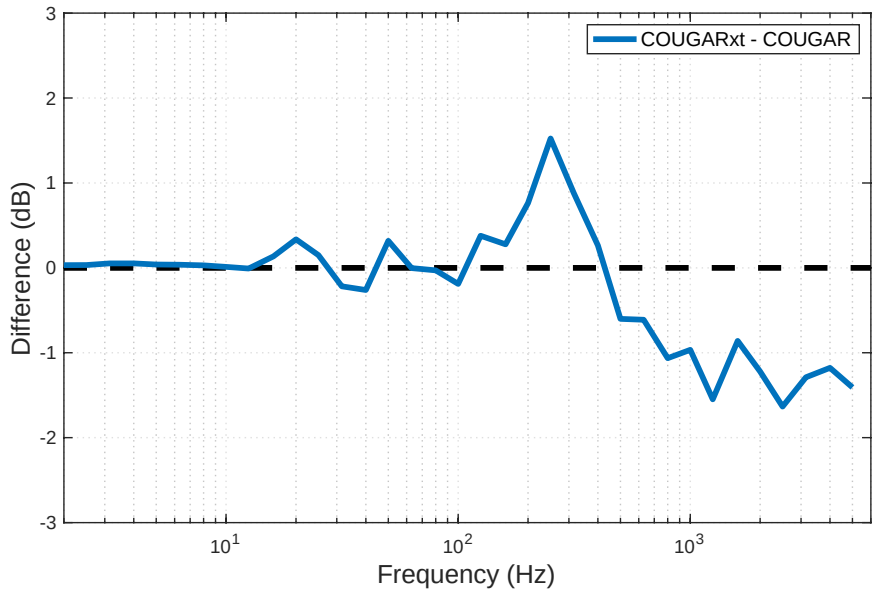

Figure 4-25. One-third octave spectral comparison between the COUGAR and COUGARxt configurations during a twenty-second segment of a GEM-63 rocket motor test. Data are only shown up to 5 kHz because that is where the signal hit the noise floor.

4.4.3. Falcon-9 Launch and Stage-1 Landing

Conversations with NASA resulted in attempts to locate sonic boom measurement opportunity prior to QSF18. On extremely short notice, two students traveled to Lompoc, CA in October, 2018 to record a SpaceX Falcon 9 launch and booster reentry that took place at nearby Vandenberg Air Force Base. The launch provided an additional opportunity to observe system noise floor and low-frequency response, but the focus was measuring the high-amplitude reentry sonic boom. The sonic boom from the booster reentry was markedly different than those measured at QSF18, but still served as a good test of the COUGAR and PUMA systems.

Two stations were deployed to record the events using various combinations of data acquisition modules and both GRAS microphones. Along with the module combinations, various positions of microphones were analyzed. For one measurement station, as seen in Figure 4-26, four COUGARs, one ground microphone, and one microphone on a tripod 1.5 m (5 feet) in the air were deployed. This setup, referred to as the North Field location, was about 400 m (0.25 mi) from the West Field location that consisted of a similar setup. Only the North Field data are discussed here.

Figure 4-26. Photo of North Field recording location. The launch occurred over the mountains, roughly marked by the red arrow. Six microphones were set up: four COUGAR-configured microphones, one microphone on the ground, and one microphone at 1.52 m (5 ft) off the ground.

The first result of the test was not acoustic, rather it was a test of system robustness. Because we learned of the planned Falcon 9 first stage landing only a few days before the test, gathering and packing the equipment had to be a quick and efficient process. All equipment was packed in two large Husky® rolling totes (that we later used at QSF18) and was brought on the plane as checked baggage. Upon arrival at the fields, equipment was quickly set up and worked perfectly. The main takeaway was that the COUGAR and PUMA systems were portable and practical.

The principal launch event of the Falcon 9 takeoff lasted 90 seconds, but low rumbles could be heard for up to 2 minutes after the main sound died off. Levels peaked around 120 dB, with an OASPL of 113 dB at steady state. The time waveforms of the launch event for each microphone are shown in Figure 4-27. The waveforms are consistent with only a slight time delay due to differences in deployment location.

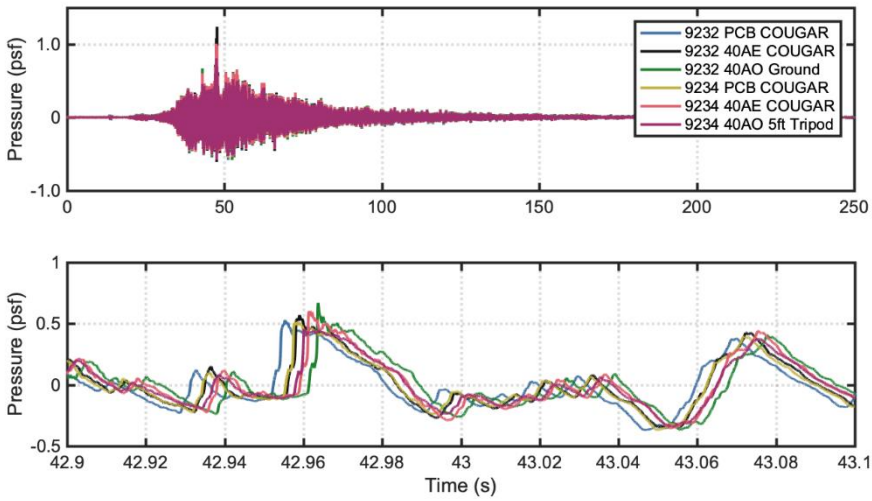

Figure 4-27. Time waveforms of the Falcon 9 launch recorded at the station seen in Figure 4-26. The lower plot is an enlarged portion of the waveform in the top plot.

The one-third octave spectra from the Falcon 9 launch shown in Figure 4-28 demonstrate that results from this test are comparable to those from the GEM-63 tests shown in Figure 4-24. The microphone and module combination with the lowest noise floor was the GRAS 40AE on the NI 9234 DAQ module. On the other hand, the combination with the best low-frequency response was the PCB 378A07 microphone on the NI 9232 DAQ module. The low-frequency response was up to 7 dB higher at 1 Hz for the PCB/NI 9232 than the GRAS/NI 9234 combination. The difference in the noise floor between the two extremes (NI 9232 COUGAR vs. NI 9234 40AE COUGAR) was approximately 60 dB at a frequency of 20 kHz. Of note, a broad interference null is apparent around 250 Hz for the 1.5 m (5 ft) raised microphone, which is expected given the placement geometry and moving source. These spectral results help confirm the potential issues with accurate sonic boom waveform recordings: the deployed setups with the lowest noise have the poorest low-frequency response. Note that this conclusion applies to the setups tested, as candidates for the QSF18 PUMA setups, and potentially not to every possible commercially-available data acquisition system and microphone configuration.

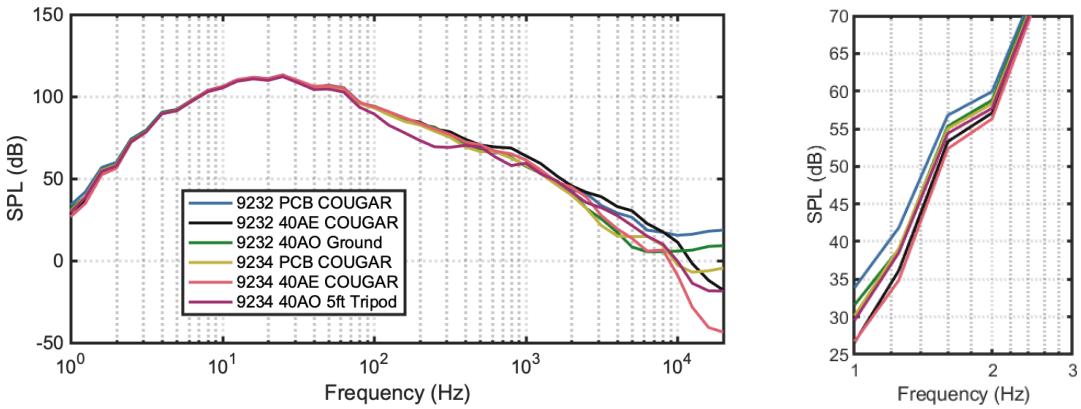

Figure 4-28. One-third octave band spectra of the launch event for each configuration. Calculations were made with 20 seconds of quasi-steady-state data during the launch. The right spectrum shows an exploded view of the 1-3 Hz range.

The sonic boom portion of the waveform shown in Figure 4-29, created by the launch vehicle's first stage reentry, shows the temporal effects of microphone and ADC module low-frequency limitations. Relative to the NI 9232/PCB 378A07 microphone, which has the best low-frequency response and yields the most linear expansion in the time interval from 0.05 to 0.23 seconds, all other channels show appreciable waveform distortion (drooping) in this interval after a similar peak overpressure. The GRAS 40AE microphone on the NI 9234 DAQ module exhibits the most droop in this interval, as expected due to the low frequency roll-off of the hardware. As a reminder, however, this combination has the lowest noise floor. Note also that the GRAS 40AE/NI 9234 channel experienced minor clipping of the peak overpressure near 0.05 seconds.

Overall, the results of the Falcon 9 measurement show that BYU was able to quickly pack, ship, and configure hardware to record a sonic boom event, with predictable limitations or differences on low-frequency response and noise floors for the different channels. While this was a markedly different sonic boom than a low-amplitude QSF18 boom, it was a good exercise in measurement and deployment techniques that proved useful during the first day of QSF18 testing.

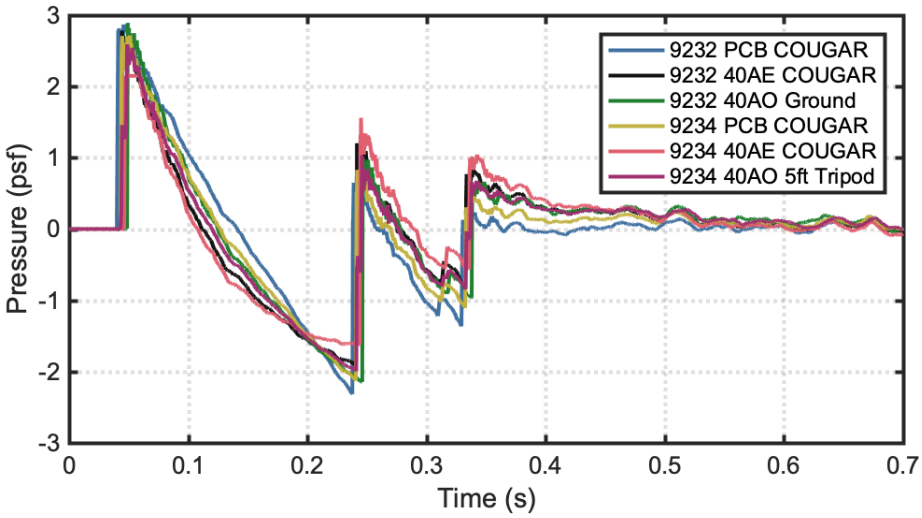

Figure 4-29. Time waveforms of the Falcon 9 booster reentry sonic boom. The ground-based GRAS 40AE microphone clipped, but the shape is still relevant in pole-shifting efforts (see Section 5.7.7).

4.4.4. COUGAR vs. COUGARxt: Wind Noise Rejection

The laboratory tests documented in section 4.3 were focused on determining the acoustical performance of the outdoor measurement systems. However, the primary purpose of the COUGAR windscreen is to reduce wind noise at the microphone, with the added benefit of preventing precipitation from reaching the microphone. One of the motivations for refining the COUGAR system came from QSF18, where high winds resulted in reduced signal-to-noise ratios at low frequencies. This led to the present COUGARxt design, whose fabrication was completed shortly before the CarpetDIEM measurement campaign. Because of generally low winds at CarpetDIEM, it was difficult to compare COUGAR and COUGARxt for wind noise rejection. Consequently, a separate test was carried out near the Provo Municipal Airport with average wind speeds around 10 m/s during the test. Both configurations, shown in Figure 4-30, used a GRAS 47AC microphone with data collected over forty minutes. The wind speed was sufficient that it dominated the noise from all acoustic sources below 100 Hz. Consequently, the difference spectrum shown in Figure 4-31 illustrates the difference, in decibels, that was observed between COUGARxt and COUGAR setups between 2 and 140 Hz during these measurements. The results show a broadband reduction in wind noise from 3 Hz to 100 Hz, with about a 4 dB reduction around 15 Hz.

Figure 4-30. The setup for testing COUGAR (far) and COUGARxt (near) under high-wind conditions. The wind direction in this image is right to left. The closer of the two setups is COUGARxt.

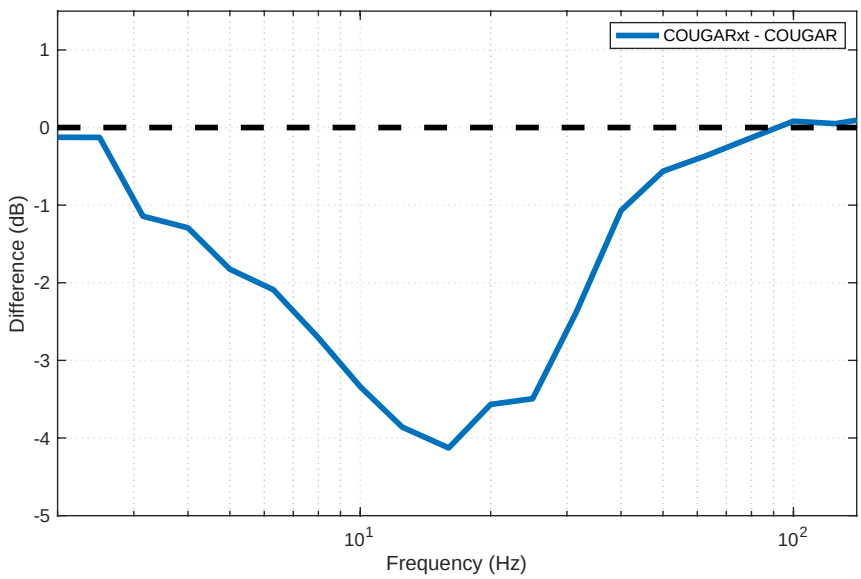

Figure 4-31. The results of the wind comparison between COUGARxt and COUGAR, demonstrating that COUGARxt has superior wind noise rejection capability relative to COUGAR.

5. QSF18 Measurement Campaign

5.1. Objectives and Findings

The objectives of BYU participation in QSF18 were to

- Test the performance of COUGAR in a quiet sonic boom environment with wind and high likelihood of precipitation
- Compare performance of different data acquisition modules and microphone combinations

- Compare performance of different microphone configurations
- Augment the number of overall stations at the QSF18 test
- Collect data to test the performance of a post-processing digital filtering technique to correct for system low-frequency response limitations

Ultimately, four stations were instrumented, with each station consisting of a setup that allowed for comparison of different data acquisition modules, microphones, and microphone configurations. During the process, the COUGAR was shown to be both weather-robust and to have lower wind noise levels than the Ground-Board and the Elevated microphone configurations meant to mimic microphone configurations used by NASA and Gulfstream at QSF18. Comparisons between different microphones and DAQ modules have resulted in an ability to pole-shift channels to improve their low-frequency responses while taking advantage of their low-noise characteristics, as will be discussed in Section 5.7.

5.2. Station Design

5.2.1. Overview

Table 5-1 and Figure *5-1* show the locations of the four BYU measurement stations at QSF18. BYU-alpha and BYU-spike1 are so named because of their collocation with Gulfstream station "alpha" at Scholes Airport and NASA station "spike 1" inside Calvary Cemetery. BYU-1 was located in Menard Park and BYU-2 was located in the U.S. Postal Service office parking lot in downtown Galveston.

At each station, the PUMA data acquisition system (overview provided in Section 4.2.1) was configured with an NI 9174 four slot USB chassis with three modules: a three-channel NI 9232 module, a two-channel NI 9250 module, and a four-channel NI 9234 module. Each of these modules has relative strengths and weaknesses, but of particular note is that the NI 9232 module has the best low-frequency response but highest noise floor, and the NI 9250 has the lowest noise floor. The NI 9234 is the same module that is used in the Gulfstream Sonic Boom Unattended Data Acquisition System (SBUDAS).[iv,v] The microphones used at each station and their configurations varied across stations, but the sampling rate used at all stations was 25.6 kHz. This sampling rate was selected because it balanced a lower noise floor (-2.5 dB relative to a sampling rate of 51.2 kHz for the NI 9232) with adequate measurement bandwidth. Although there was some concern that this does not allow for full measurement of the 12.5 kHz one-third octave band (the highest band present in Perceived Level (PL) calculations), QSF18 data analysis shows that the effective measurement bandwidth for the booms is far lower.

Two other items of note are related to the PUMA configuration for QSF18. First, pass-through solar charging was used because heat inside the case was not a concern. Despite the cloudy, rainy weather, the solar panels were able to keep the lithium-ion power banks nearly fully charged. Second, the IRIG-B GPS time clocks were not purchased and available for BYU stations at QSF18. Thus, BYU data are not GPS time-synced to other QSF18 stations. This limits the accuracy of comparing boom arrival times.

Table 5-1. Identifiers and locations of the four BYU measurement stations at QSF18.

BYU Station	Location Name	Latitude	Longitude
BYU-alpha	Fire Station #4	29°16'3.06"N	94°51'16.37"W
BYU-spike1	Calvary Cemetery	29°16'17.76"N	94°49'57.95"W
BYU-1	Menard Park	29°17'17.65"N	94°47'35.75"W
BYU-2	US Post Office	29°18'10.25"N	94°47'38.08"W

Figure 5-1. A portion of Galveston Island with the four BYU QSF18 measurement stations marked.

Figure 5-2 provides an overview of the three microphone configurations that were compared as part of QSF18: COUGAR, Ground-Board, and Elevated. COUGAR is the system tested under this program, whereas the other two systems are similar to those used by NASA and by Gulfstream for sonic boom testing. The Elevated microphone is similar to Gulfstream's SBUDAS setup for QSF18, which has a microphone pointed skyward (for free-field type measurements), located approximately 0.46 m (18 in) off the ground. The Ground-Board microphone configuration is similar to that used with SPIKE, NASA's sonic boom measurement system deployed at QSF18.[vi] SPIKE uses microphones laid beneath half-ball windscreens on plywood ground boards, which has been NASA's standard microphone configuration for sonic boom testing for over a decade. Note that the location of the microphone on the ground board (centered vs. offset) was not prescribed in our setup, but all laboratory and field testing have shown that any effect is minor. This is similar to the COUGAR plate tests shown in Section 4.3 and 4.4. These three setups are discussed frequently as part of the QSF18 and CarpetDIEM testing.

COUGAR	Ground-Board	Elevated
16” Diameter UHMW Plate	2’ x 2’ Plywood Board	Small Tripod
1.5” Thick Windscreen	Half-Ball Windscreen	GRAS AM0052 Windscreen
Microphone inverted ¼” above Plate	Microphone laid horizontal on board	Microphone mounted 18” above ground

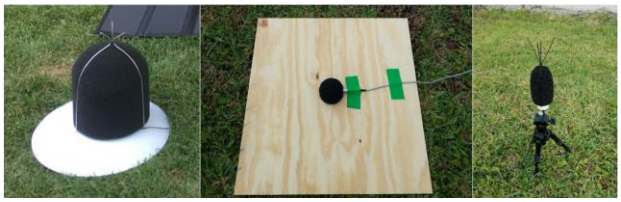

Figure 5-2. Description of the COUGAR, Ground-Board, and Elevated stations. The Ground-Board setup is intended to mimic NASA’s SPIKE stations and the Elevated setup is intended to mimic Gulfstream Aerospace’s SBUDAS microphone configuration.

5.2.2. BYU-alpha

This station serves as a comparison of COUGAR, Ground-Board, and Elevated microphone configurations, as well as a possible future direct comparison to the Gulfstream-alpha site. There were three COUGAR configurations set up with different combinations of microphone and module. Additionally, there were two Ground-Board configurations with identical microphones but different modules. An Elevated configuration was also used for comparison against the COUGAR and Ground-Board configurations.

The data acquisition module, microphone type, and its configuration for the six channels at BYU-alpha are shown in Table 5-2. Photographs are shown in Figures 5-3 and 5-4. The location was immediately adjacent to Scholes airport, and was also near a small roadway with occasional vehicle traffic. The microphones were placed on an open, grassy area adjacent to the road and a fenced-in parking area.

Table 5-2 - Configuration for BYU-alpha station, where three different data acquisition modules were used. COUGAR, Ground-Board and Elevated microphone configurations were compared at this station.

CH#	Module	Mic	Config
0	NI 9232	PCB 378A07	COUGAR
1		B&K 4193	Ground-Board
2		GRAS 47AC	COUGAR
3	NI 9250	GRAS 40AE	COUGAR
4		B&K 4193	Ground-Board
5	NI 9234	GRAS 46AN	Elevated

Figure 5-3. Several perspectives on the BYU-alpha station showing COUGAR, Ground-Board, and Elevated microphone configurations. [Upper Right] A photograph of the local data acquisition system

Figure 5-4. A view of the BYU-alpha station showing all of the different microphone configurations on the right and the data acquisition equipment on the left.

5.2.3. BYU-spike1

As described in Table 5-3 and Figures 5-5 and 5-6, this station serves as a comparison for COUGAR using different microphones and modules. A Ground-Board configuration was also included on the same module as one of the COUGARs. The microphone configurations were all placed in a straight line. The microphones were in an open, grassy area with a concrete mausoleum approximately 10 m (~30 ft) from the microphones. The mausoleum may eventually be of interest for examining reflections off a single building. This station was also collocated with a NASA-operated SPIKE station.

Table 5-3. Configuration for the BYU-spike1 station. Two different data acquisition modules were used. COUGAR and Ground-Board microphone configurations were compared at this station.

CH#	Module	Mic	Config
0	NI 9232	PCB 378A07	COUGAR
1		GRAS 46AO	Ground-Board
2	NI 9250	GRAS 40AE	COUGAR
3		GRAS 46AO	COUGAR

Figure 5-5. [Left] A worker operates on the configurations located at BYU-spike1. [Right] A full view of the microphone configurations, data acquisition system, and solar power unit at BYU-spike1.

Figure 5-6. A full view of the BYU-spike1 station. The SPIKE configuration shown in the bottom left was operated by NASA while the Ground-Board configuration in the center of the frame was operated by BYU.

5.2.4. BYU-1 (Menard Park)

This station serves as a comparison for COUGAR, Ground-Board, and Elevated microphone configurations using different microphones and modules. The microphones were in an open, grassy area in Menard Park. In addition to fairly regular traffic, the noise from the amusement park on the pier was audible, as were activities from family gatherings at the nearby pavilion. Table 5-4 describes the PUMA configuration, microphone types, and their configurations. Photographs of the setup, as well as the solar charging panel, are shown in Figures 5-7 and 5-8. Note that the Elevated setup in this case was accomplished by mounting a GRAS 46AO pressure-field microphone horizontally off the Kestrel weather station tripod, so as to be at grazing incidence, at a height of 0.46 m (18 in).

Table 5-4. Configuration for BYU-1 station. Three different data acquisition modules were used. COUGAR, Ground-Board, and Elevated microphone configurations were compared at this station.

CH#	Module	Mic	Config
0	NI 9232	PCB 378A07	COUGAR
1		GRAS 46AO	Ground-Board
2	NI 9250	GRAS 40AE	COUGAR
3		GRAS 46AO	Ground-Board
4	NI 9234	PCB 378A07	COUGAR
5		GRAS 46AO	Elevated

Figure 5-7. Two views of the BYU-1 station.

Figure 5-8. [Left] A view of the BYU-1 station showing the microphone configurations, data acquisition equipment and the solar power unit. [Right] An example of a worker at the BYU-1 station.

5.2.5. BYU-2 (US Post Office)

This station serves as a comparison for COUGAR and Ground-Board using different microphones and modules, as shown in Table 5-5. The microphones were in the parking lot of a post office, placed on a hard and acoustically reflective asphalt surface, as shown in Figure 5-9. The parking lot was surrounded by buildings and was in a relatively urban portion of the test area compared to other sites. Future analysis of these and other urban data may be of interest.

Table 5-5. Configuration for BYU-2 station. Three different data acquisition modules were used. COUGAR and Ground-Board configurations were compared at this station.

CH#	Module	Mic	Config
0	NI 9232	PCB 378A07	COUGAR
1		GRAS 46AO	Ground-Board
2	NI 9250	GRAS 40AE	COUGAR
3		GRAS 46AO	Ground-Board
4	NI 9234	GRAS 46AO	Ground-Board

Figure 5-9. [Left] A view of the BYU-2 station showing the microphone configurations. This station was different from the others because the microphones were placed on a hard surface. [Right] A photograph of a Kestrel portable weather device used to acquire weather data during the tests.

5.3. Campaign Logistics

The BYU measurement team began collecting data in the early morning on 8 November 2018, a few days after the start of QSF18. The weather proved to be an overall challenge to the measurement campaign but represented an ideal opportunity to evaluate the robustness of COUGAR. Four sonic booms (booms 18-21) from two flights were recorded on 8 November. Three stations (BYU-alpha, BYU-spike1, and BYU-1) were set up. Thirteen sonic booms (booms 22-34) from three flights were recorded on 10 and 11 November. All four stations were set up, with BYU-2 being active after Boom 23. The BYU measurement team departed on November 13th, but provided a two-COUGAR version of the BYU-alpha setup for Dr. Alexandra Loubeau (NASA) to set up and record unattended. Five sonic booms (booms 35-39) were recorded with this setup.

5.4. Summary of Booms Recorded

Table 5-6 shows a summary table for sonic booms 18-39, for which BYU systems were deployed. On the first day (booms 18-23), BYU-2 was not deployed. On the last day, only a portion of BYU-alpha was

deployed and set to trigger automatically throughout the day. Amplitude-based triggering was successful in all but two cases: Boom 22 at BYU-spike 1 (failure to set trigger) and Boom 29 at all BYU stations (trigger failure due to low amplitude). A damaged cable was responsible for the "hardware error" at BYU-2's channel 0.

Table 5-6. Summary of sonic boom recording success for BYU stations for sonic booms 18-39. Green – successfully recorded data. Red – no data. "X" – Hardware wasn't deployed. "T" – Trigger not properly set. "B" – Boom was inaudible. "H" – Hardware error.

		LOCATION/ CHANNEL																				
		BYU-alpha						BYU-spike1				BYU-1						BYU-2				
		0	1	2	3	4	5	0	1	2	3	0	1	2	3	4	5	0	1	2	3	4
Boom	18																	X	X	X	X	X
	19																	X	X	X	X	X
	20																	X	X	X	X	X
	21																	X	X	X	X	X
	22							T	T	T	T							X	X	X	X	X
	23																	X	X	X	X	X
	24																					
	25																					
	26																					
	27																					
	28																					
	29	B	B	B	B	B	B	B	B	B	B	B	B	B	B	B	B	B	B	B	B	B
	30																	H				
	31																	H				
	32																	H				
	33																	H				
	34																	H				
	35		X	X		X	X	X	X	X	X	X	X	X	X	X	X	X	X	X	X	X
	36		X	X		X	X	X	X	X	X	X	X	X	X	X	X	X	X	X	X	X
	37		X	X		X	X	X	X	X	X	X	X	X	X	X	X	X	X	X	X	X
	38		X	X		X	X	X	X	X	X	X	X	X	X	X	X	X	X	X	X	X
	39		X	X		X	X	X	X	X	X	X	X	X	X	X	X	X	X	X	X	X

5.5. Boom Metrics

As previously described in Section 5.2, each location had an NI 9250 module paired with a 40AE microphone inside a COUGAR configuration, which provided the highest SNR and provided the highest-fidelity channel for boom metric calculations. This channel was used to calculate the Perceived Level (PL), six different weighted Sound Exposure Levels (SEL) – Z, A, B, C, D, E – and Indoor Sonic Boom Annoyance Predictor (ISBAP). The calculated metrics (using a 650 ms time window) are shown for the four BYU stations Tables 5-7 through 5-10. There are two items of note: First, these metrics were calculated after the pole-shifting process described in Section 5.7. Second, as described in Section 0, the sonic boom metric values are impacted by the limited measurement bandwidth. Development of a consistent procedure to calculate boom metrics over the frequency range of interest is an important topic of future research.

Table 5-7. Metrics for the booms recorded at BYU-alpha.

		BYU-alpha							
		PL	ZSEL	ASEL	BSEL	CSEL	DSEL	ESEL	ISBAP
Boom	18	72.4	101.9	59.2	74.4	87.4	75.6	69.6	84.2
	19	73.5	106.1	58.9	76.2	89.7	77.7	70.7	86.5
	20	72.5	103.5	59.0	74.7	88.8	76.6	69.7	85.0
	21	85.3	109.4	71.7	85.6	96.1	85.4	81.3	95.5
	22	71.7	102.3	57.2	73.5	87.8	75.4	68.3	84.5
	23	76.1	106.0	62.6	76.6	87.4	77.8	72.4	86.6
	24	71.7	98.7	57.7	73.5	84.0	73.3	68.6	82.7
	25	75.2	104.4	60.9	77.7	90.8	78.6	72.4	87.7
	26	82.3	108.7	69.3	82.5	93.8	83.0	78.5	92.6
	27	75.8	109.2	61.2	78.9	93.2	81.0	73.3	89.2
	28	81.0	107.7	66.2	82.5	94.4	82.8	77.4	92.8
	30	73.8	105.9	60.1	75.0	86.8	76.5	70.3	85.0
	31	72.1	102.8	58.2	73.2	86.4	74.5	68.4	83.9
	32	74.0	100.7	60.1	75.9	87.7	75.9	70.8	85.6
	33	82.8	105.4	70.2	82.0	93.0	82.2	78.3	92.4
	34	68.1	101.4	53.8	71.9	87.7	74.7	66.1	82.3
	35	75.1	108.4	60.3	76.6	92.5	80.2	71.5	88.6
	36	78.9	107.8	64.5	79.3	92.2	80.6	74.6	90.6
	37	86.1	110.0	71.9	85.8	99.5	87.0	81.1	97.7
	38	71.4	103.3	56.6	73.2	86.8	75.2	67.8	84.1
	39	68.7	103.2	53.6	70.5	87.5	75.0	65.1	82.9

Table 5-8. Metrics for the booms recorded at BYU-spike1.

		BYU-spike1							
		PL	ZSEL	ASEL	BSEL	CSEL	DSEL	ESEL	ISBAP
Boom	18	73.7	99.8	60.6	74.9	85.8	75.0	70.7	84.3
	19	83.2	108.1	70.2	83.7	93.7	83.5	79.6	93.0
	20	72.2	103.3	58.8	74.3	87.6	75.8	69.5	84.3
	21	83.7	109.8	69.6	83.8	95.2	84.2	79.4	94.5
	23	74.4	102.0	60.6	76.4	88.8	76.9	71.4	86.3
	24	74.2	100.7	60.0	74.7	86.6	75.3	70.0	85.4
	25	75.9	104.7	61.8	77.7	90.6	78.8	72.7	88.0
	26	76.8	109.4	63.0	78.7	92.9	81.0	73.7	89.4
	27	81.6	110.6	67.3	82.9	95.6	83.9	78.0	93.5
	28	72.4	105.0	59.4	74.8	86.8	75.9	70.0	84.0
	30	75.1	102.5	61.7	76.0	86.3	76.0	71.7	85.4
	31	71.9	107.6	60.3	75.0	89.4	78.1	70.5	84.1
	32	72.8	105.8	59.0	75.0	87.7	76.0	69.9	84.8
	33	89.2	109.2	74.5	87.7	98.4	87.6	83.6	99.3
	34	72.1	103.8	58.4	75.1	88.6	76.2	69.7	84.8

Table 5-9. Metrics for the booms recorded at BYU-1.

		BYU- 1							
		PL	ZSEL	ASEL	BSEL	CSEL	DSEL	ESEL	ISBAP
Boom	18	72.4	103.3	57.4	71.6	85.8	74.1	67.0	84.3
	19	87.6	111.0	72.1	88.3	100.2	88.4	83.2	99.4
	20	73.7	106.1	59.2	71.8	85.0	74.5	67.8	84.6
	21	87.6	109.4	73.9	86.7	97.6	86.7	82.8	97.6
	22	74.3	104.0	58.7	74.8	89.1	77.0	69.5	87.1
	23	78.0	103.4	65.6	74.6	86.2	76.0	71.8	86.7
	24	76.2	101.6	62.7	74.3	86.8	75.4	70.0	86.3
	25	75.0	100.0	61.3	72.2	85.2	73.7	68.1	85.1
	26	81.4	108.5	66.9	79.5	91.7	80.9	75.4	91.8
	27	92.9	113.7	80.7	91.4	99.1	90.9	88.5	100.6
	28	84.5	110.4	69.3	84.3	96.9	85.0	79.3	96.1
	30	76.0	104.5	60.9	75.1	88.4	76.8	70.4	87.6
	31	81.0	109.5	66.4	79.7	92.1	81.0	75.5	91.8
	32	75.1	99.8	60.4	72.0	84.8	73.4	68.1	85.3
	33	83.1	107.9	68.2	81.0	91.1	81.2	77.2	92.8
	34	77.6	106.3	62.6	77.0	90.3	78.7	72.2	89.2

Table 5-10. Metrics for the booms recorded at BYU-2.

		BYU- 2							
		PL	ZSEL	ASEL	BSEL	CSEL	DSEL	ESEL	ISBAP
Boom	24	74.7	101.8	59.7	76.2	90.4	77.7	70.7	87.5
	25	70.6	98.9	58.2	67.3	80.5	69.9	63.9	79.9
	26	77.0	107.5	63.6	77.4	91.2	79.6	72.9	88.6
	27	83.1	112.2	68.5	83.4	95.3	84.3	78.7	94.3
	28	88.3	110.1	74.4	88.0	98.7	87.8	83.7	98.5
	30	77.8	104.7	63.6	79.3	91.5	79.9	74.3	89.5
	31	86.7	107.1	72.5	86.2	97.0	86.0	81.9	97.0
	32	72.7	98.4	58.3	71.2	83.4	72.0	66.7	83.3
	33	86.1	104.9	72.2	86.0	95.4	85.2	81.7	95.8
	34	75.5	104.4	61.0	75.2	90.5	78.1	70.4	87.9

5.6. Data Analysis

5.6.1. Ambient Spectra at BYU Stations

Shown in Figure 5-10 are example ambient spectra at all four BYU stations preceding four booms. In each case, the low-frequency levels (below ~20 Hz) are the greatest at BYU-alpha (airport) and BYU-spike1 (cemetery). As shown in the pictures for each setup, these locations were the least sheltered from the wind. At high frequencies, BYU-1 had the greatest levels, which are likely due to the nearby presence of the amusement park and vehicle traffic.

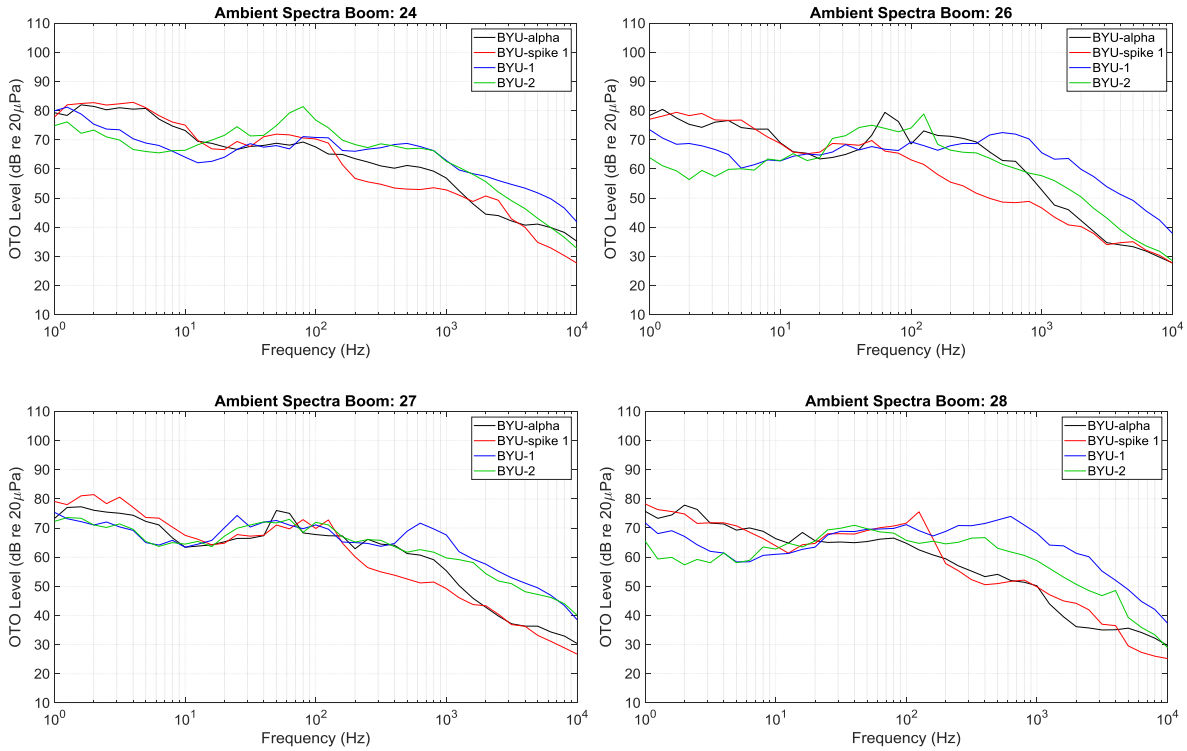

Figure 5-10. Ambient spectra at the BYU stations for the 60-second period preceding booms 24, 26, 27, and 28. The low-noise, NI 9250/GRAS 40AE channel was used for each case.

5.6.2. Example Waveforms at BYU Stations

Displayed in Figure 5-11 are the four booms for which the ambient spectra were shown in Figure 5-10, at all four BYU measurement stations. To most accurately visualize the N-wave shape, the booms in these figures are shown as recorded by the NI 9232 module and the PCB 378A07 microphone because this system has the best low-frequency response of the BYU hardware combinations. The purpose in showing these four booms is to point out the kinds of measurement differences seen at different stations and for different booms (from different flight trajectories), suggesting avenues for future analyses. For example, Boom 24 at BYU-2 has the largest peak overpressure of any of the four stations and has a greater amount of ringing post-boom. While this might be thought to be due to reflections off buildings in the downtown Galveston area, examination of other booms, like Boom 26, shows this is not consistent. On the other hand, Boom 27 shows turbulence-like peakedness in the bow shock at BYU-1, whereas Boom 28 shows a double set of booms at BYU-1 and BYU-2, but not at the other two stations. In any event, few booms have the relatively clean shape of Boom 26, that was remarkably similar across all four stations.

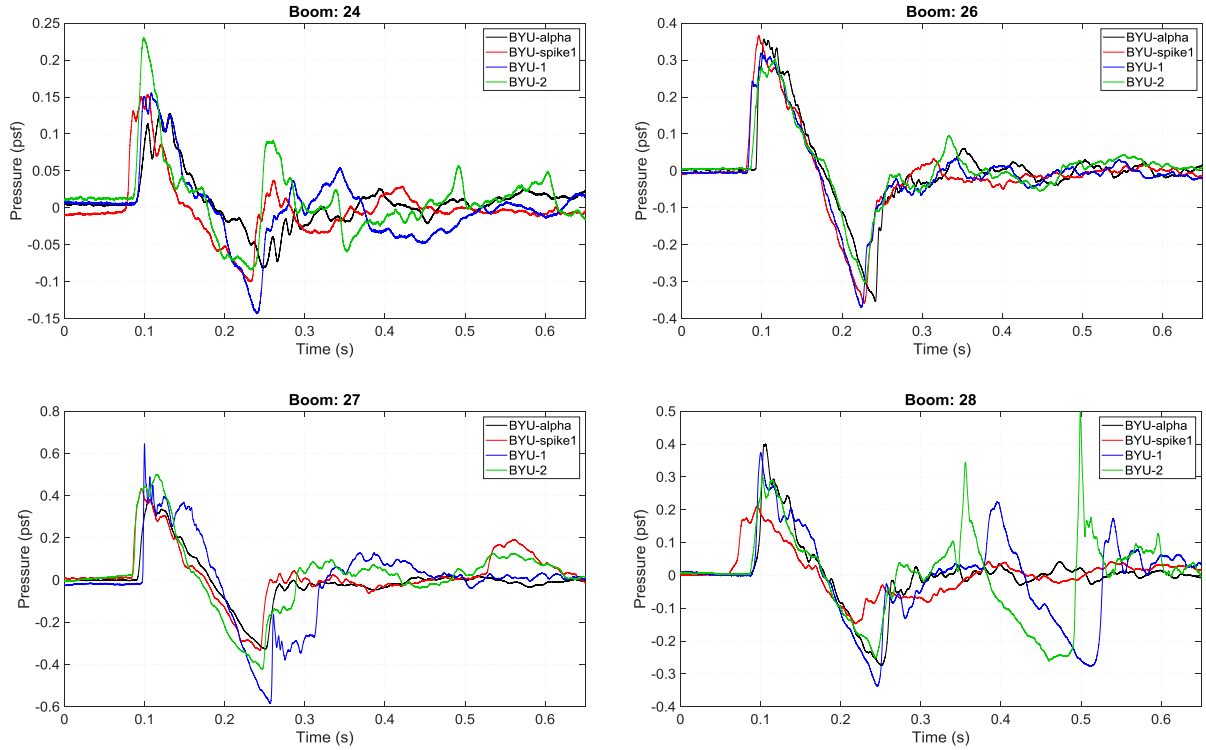

Figure 5-11. Booms 24, 26, 27, and 28 over a 650 ms time window at all four BYU stations. Booms have been aligned according to initial peak overpressure. Shown are the recordings from the channels with the best low-frequency response: the NI 9232/PCB 378A07.

5.6.3. BYU-Alpha Analysis

To understand the impact of DAQ module type, microphone type, and microphone configuration, it is helpful to examine sample waveforms, boom spectra, and signal-to-noise ratio (SNR) spectra. The SNR spectrum is the difference, in dB, between the boom one-third octave level spectrum and the ambient level spectrum. For conciseness, only the BYU-alpha station is considered. Displayed in Figure 5-12 are the same four booms as described in Figure 5-11: 24, 26, 27, and 28 across all six channels at BYU-alpha. The differences in low-frequency response for some channels are apparent. Most noticeable is the NI 9250/40AE microphone's greater tendency to dip lower than the other microphones during the linear ramp portion of the boom, and then overshoot to positive pressures at the tail shock portion. The NI 9232/PCB 378A07 and the NI 9232/GRAS 47AC module/microphone pairs are believed to provide the most visually accurate waveform representations because they have the best low-frequency responses of any of the channels. Corrections for low-frequency response limitations of the other channels are described in Section 5.7.

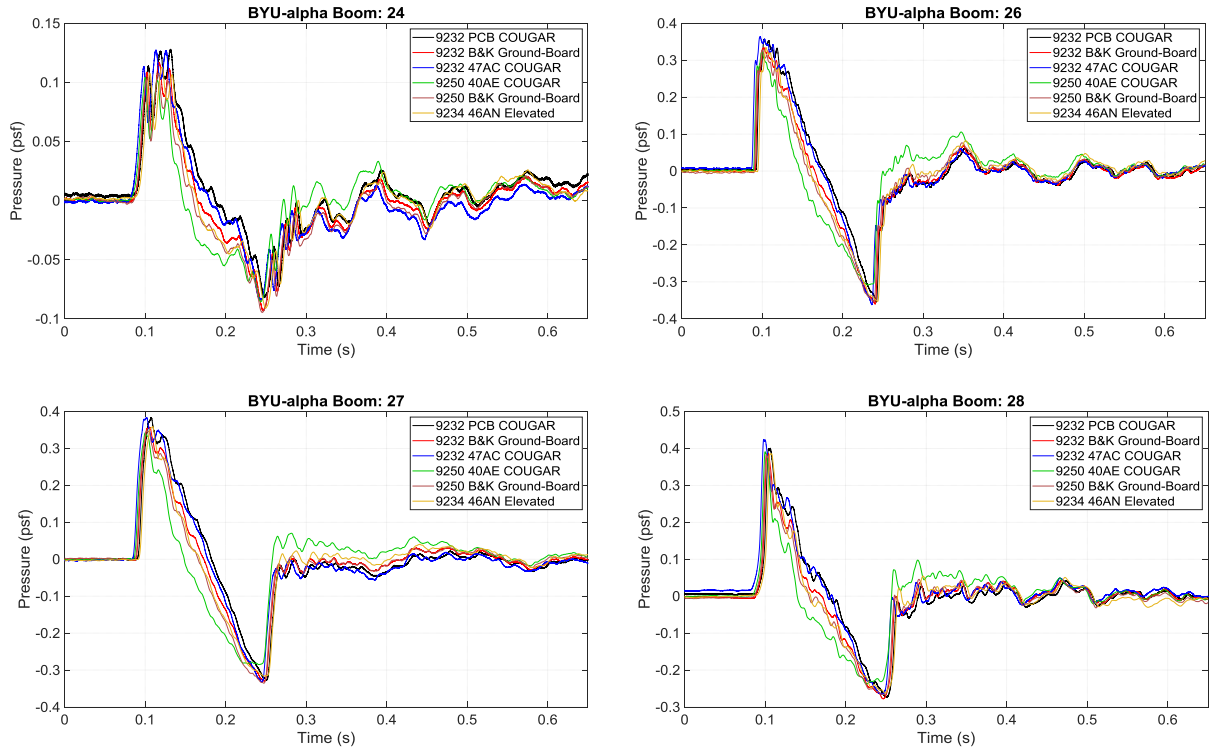

Figure 5-12. Booms 24, 26, 27, and 28 over a 650 ms time window at BYU-alpha station. Differences in shape from different hardware configurations are apparent.

One-third octave spectra for the four booms and all channels at BYU-alpha are shown in Figure 5-13. The "jaggedness" of the levels at the low-frequency bands is due to the small window size (650 ms) used to estimate the one-third octave spectrum. Note that zero-padding the waveform to improve low-frequency smoothness could be used in future analysis efforts, but standardized analysis techniques need to be developed in conjunction with NASA for consistency.

These spectra help reveal some of the important differences and limitations in the data acquisition configurations. Most notable is the challenge created by using the NI 9232. Although the NI 9232 has the best low-frequency response, its noise floor above 1 kHz may be too high for recording low-amplitude booms. The comparatively high noise floor above 1 kHz is apparent in all of the boom spectra that were recorded using the NI 9232 module in Figure 5-13. Metric levels would be artificially increased using this module, especially because many of the metrics weigh levels between 1 kHz and 5 kHz higher than other frequency bands. Use of a microphone with a greater sensitivity helps reduce the noise floor somewhat (compare red curve vs. blue), but not enough to merit the NI 9232's use. Second, in looking at the low-frequency portion of the spectra in Figure 5-13, the roll-off of the NI 9250/GRAS 40AE combination is apparent but is quite minor on this scale. Finally, of the three low-noise channels, both the NI 9250/B&K 4193 and the NI 9234/GRAS 46AN channels begin to flatten out at 10 kHz. In both cases, the system noise floor is being approached. The only channel that has the potential for a 10 kHz measurement bandwidth in these cases is the NI 9250/GRAS 40AE combination.

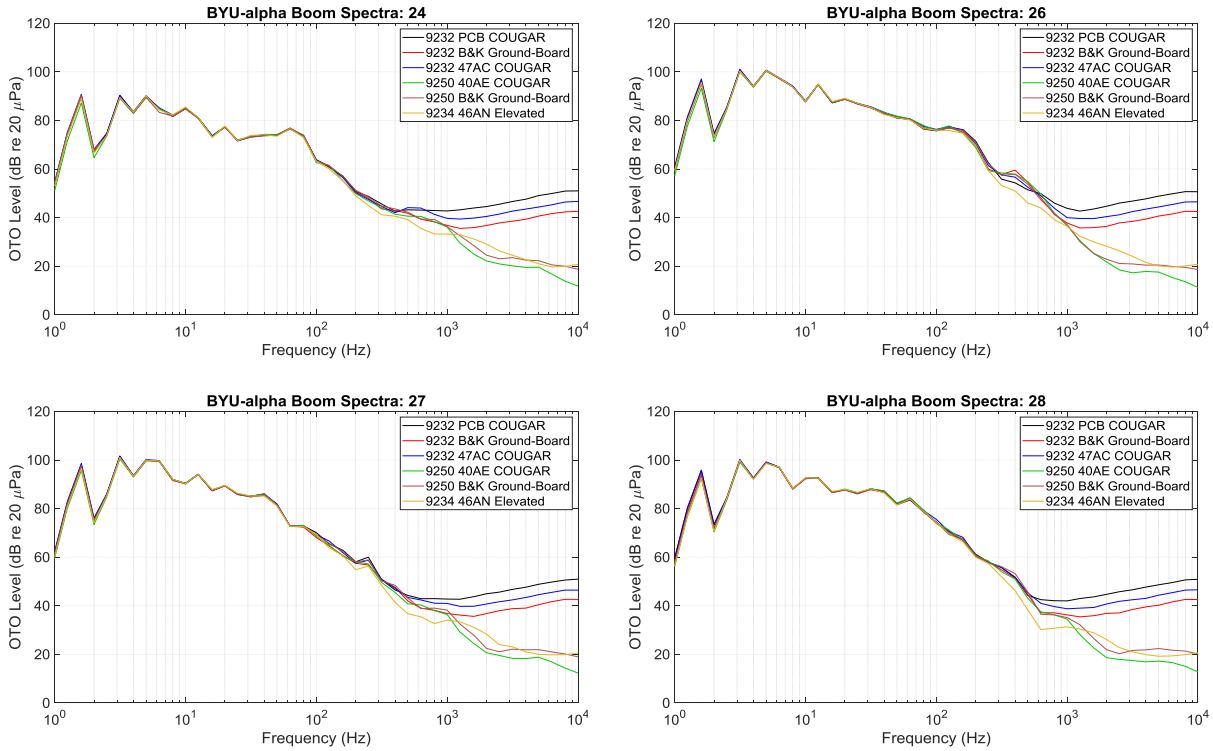

Figure 5-13. One-third octave spectra for the four booms shown in Figure 5-12.

Another plot that is useful in tandem with the boom spectra in Figure 5-13 is the SNR spectrum. The SNR spectra for the four booms and all channels at BYU-alpha are shown in Figure 5-14. This plot lends insight into the advantages and disadvantages of different configurations. Note that from Figure 5-13, all channels have nearly equivalent measured spectra between 1 and 100 Hz for the four booms shown, with the exception of slight low-frequency differences due to instrument response. However, when examining the SNR spectrum, there is a distinct ordering that occurs in each case based on microphone configuration: the Elevated configuration has the lowest SNR, followed by the Ground-Board, with COUGAR having the highest SNR. This is consistent across all booms and stations with the setups.

These differences in the low-frequency SNR spectra are due to the wind noise rejection performance of the different systems: the boom one-third octave levels are nearly identical, but the ambient spectra vary considerably. Although detailed, quantitative examination of the three setups to understand their differences in wind noise reduction has not been carried out, some comments can be made. First, the wind speed varies rapidly with height near the ground surface (where there is a no-slip condition), and an elevated microphone is subjected to greater wind speeds. Second, the wind noise reduction provided by a windscreen depends on multiple factors (size, thickness, porosity, shape, airspeed, etc.) that are still being studied.[vii,viii,ix] Two of these are the size of the windscreen and its thickness. A larger windscreen moves the microphone as far away as possible from the turbulence-induced pressure fluctuations around the screen. Second, for equal porosity, the air speed reduction through the screen increases with greater thickness.

Using these explanatory principles, the SNR ordering by the three setups can be described. First, the Elevated setup has a microphone located 0.46 m (18 in) off the ground, where wind speeds are higher, and has a smaller and thinner windscreen. All three factors work against the ability of the Elevated

microphone setup to reduce wind noise. Second, the Ground-Board configuration uses a microphone laid on the board covered by a commercial 90 mm (3.5 in) diameter spherical windscreen cut in half. Being near the ground surface, the wind speed is lower, and the windscreen is thicker than that used with the Elevated setup. This leads to improved wind noise reduction and a greater SNR. Finally, the COUGAR configuration uses an inverted microphone only slightly raised above the ground at 6.35 mm (0.25 in) above the plate apex, a windscreen thickness of 40 mm (1.5 in) and a larger overall windscreen size, resulting in greater separation between windscreen interior surface and microphone. This combination of factors results in improved wind noise reduction relative to the Ground-Board or Elevated microphone configurations and, consequently, greater low-boom SNR when there is appreciable wind. Note that for all configurations, however, the SNR decreases at low frequencies due to the combination of increased wind noise and the low signal level below 5 Hz.

An additional important point can be made using these spectra. In all four cases here (which are typical of all booms recorded), the SNR drops to around 0 dB by 1 kHz. This means that even though the NI 9250 and NI 9234 modules have greater measurement bandwidth, wind and other ambient noise still dominate the signal at high frequencies. This low measurement bandwidth can appreciably impact noise metric calculations, which is demonstrated in Section 0.

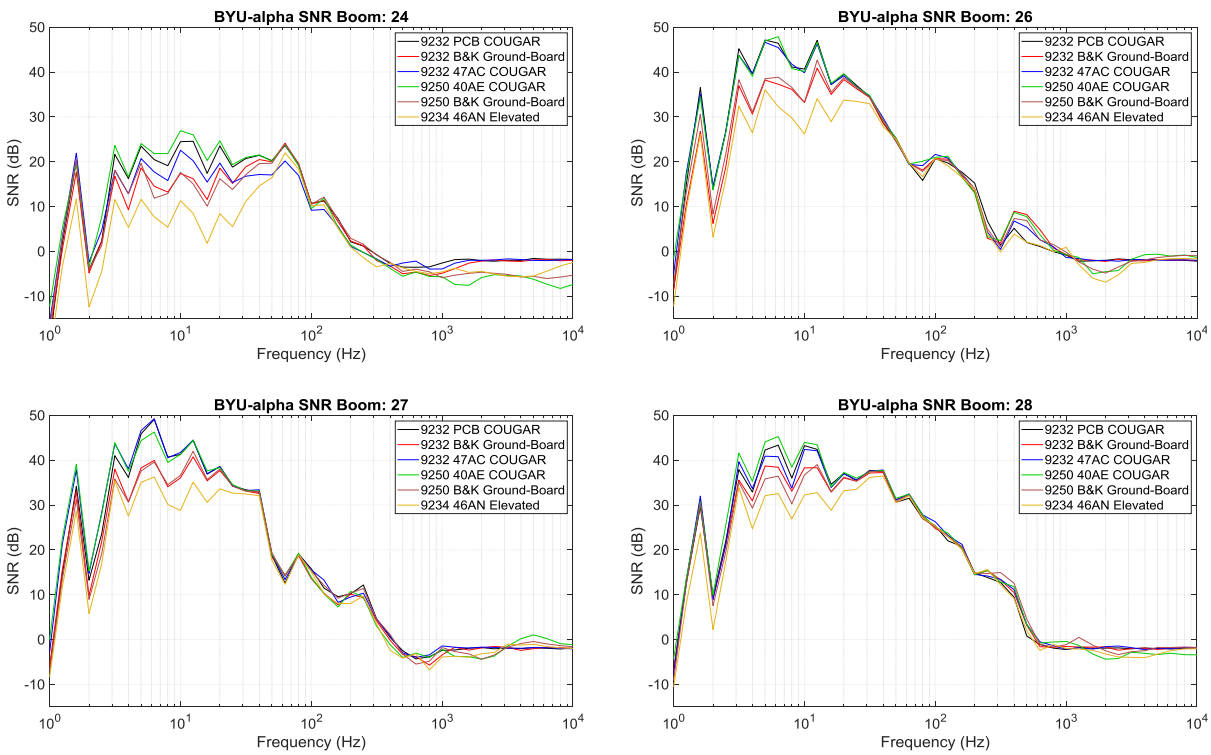

Figure 5-14. Signal-to-noise ratio (dB) spectrum for the boom relative to the ambient spectrum for the four example booms from Figure 5-12 at BYU-alpha.

5.6.4. Mean Relative Metrics

Although the aircraft waypoint and trajectory varied significantly across booms in order to vary exposure levels across the Galveston community, average differences across microphone channels can be quantified by determining a reference channel at each BYU station and calculating the average differences relative to that channel. For each station, the NI 9250/GRAS 40AE channel in the COUGAR configuration

was selected as the reference channel and the mean differences for other channels (described in Section 5.2), in dB, were calculated for Booms 18-34 (where all four BYU stations were deployed). The arithmetic means of the decibel differences are shown in Tables 5-11 through 5-14. The tables show systematic differences between setups, as described in Sections 0 and 5.6.6.

Table 5-11. Mean difference (in dB) between recordings from the NI 9250/GRAS 40AE/COUGAR channel and the other channels at BYU-alpha.

		BYU- alpha							
		PL	ZSEL	ASEL	BSEL	CSEL	DSEL	ESEL	ISBAP
CHANNEL	0	4.3	-0.3	3.0	-0.1	-0.3	0.3	1.4	2.9
	1	2.1	-0.4	0.5	-0.3	-0.3	-0.2	0.0	1.7
	2	3.3	-0.2	1.6	0.1	-0.1	0.1	0.7	2.6
	3	-	-	-	-	-	-	-	-
	4	0.1	-0.4	-0.1	-0.3	-0.3	-0.3	-0.2	0.0
	5	-1.0	-0.8	-1.1	-0.8	-0.6	-0.7	-0.9	-0.8

Table 5-12. Mean difference (in dB) between recordings from the NI 9250/GRAS 40AE/COUGAR channel and the other channels at BYU-spike1.

		BYU- spike1							
		PL	ZSEL	ASEL	BSEL	CSEL	DSEL	ESEL	ISBAP
CHANNEL	0	3.8	-1.0	2.1	-0.5	-0.6	0.0	0.8	2.7
	1	2.4	0.7	0.9	0.2	0.1	0.2	0.5	2.1
	2	-	-	-	-	-	-	-	-
	3	0.0	0.3	-0.2	-0.1	0.0	0.0	-0.1	0.1

Table 5-13. Mean difference (in dB) between recordings from the NI 9250/GRAS 40AE/COUGAR channel and the other channels at BYU-1.

		BYU- 1							
		PL	ZSEL	ASEL	BSEL	CSEL	DSEL	ESEL	ISBAP
CHANNEL	0	2.2	-0.7	1.6	0.0	-0.1	0.4	1.2	1.5
	1	1.7	0.9	1.2	0.8	0.8	0.9	1.2	1.6
	2	-	-	-	-	-	-	-	-
	3	0.0	-0.6	-0.1	-0.1	-0.2	-0.2	-0.1	0.0
	4	0.4	-0.7	0.1	-0.1	-0.2	-0.2	0.0	0.3
	5	-1.1	0.3	-1.3	-0.7	-0.4	-0.5	-0.8	-0.8

Table 5-14. Mean difference (in dB) between recordings from the NI 9250/GRAS 40AE/COUGAR channel and the other channels at BYU-2.

		BYU- 2							
		PL	ZSEL	ASEL	BSEL	CSEL	DSEL	ESEL	ISBAP
CHANNEL	0	3.3	-0.7	1.6	0.0	-0.1	0.4	1.2	1.5
	1	1.7	0.9	1.2	0.8	0.8	0.9	1.2	1.6
	2	-	-	-	-	-	-	-	-
	3	0.0	-0.6	-0.1	-0.1	-0.2	-0.2	-0.1	0.0
	4	0.4	-0.7	0.1	-0.1	-0.2	-0.2	0.0	0.3

5.6.5. Impact of DAQ module on Mean Metrics

Tables 5-11 through 5-14 show that some metric levels of booms recorded on channels using the high-noise NI 9232 module are substantially higher than for the low-noise reference channel. The metrics that are most affected by the high electronic noise levels (shown above 1kHz in Figure 5-13) are PL, ASEL, ESEL, and ISBAP.

However, the problem with measurement and bandwidth is not limited to the measurements made using the NI 9232 module. The limited SNR above 1 kHz has an impact on all the low-boom measurements. Figure 5-14 showed that the SNR at BYU-alpha was only positive (above the ambient or electronic noise floor) below 1 kHz. Given the relative importance that frequencies above 1 kHz have in some of the metric calculations, sonic boom levels could be biased high by the ambient noise included in the calculation.

As a simple example of this possibility, several boom waveforms were low-pass filtered (using a fourth-order Butterworth filter) to only include the frequencies where the SNR was positive, and PL was recalculated. For those booms that had a bandwidth up to around 1 kHz, the effect of low-pass filtering was minor, reducing the PL by approximately 0.5 – 1 dB. However, for those booms whose bandwidth was less than 500 Hz, the impact of filtering was much greater, reducing the PL by 2 – 4 dB. The ISBAP metric, which relies on PL, was similarly impacted.

Note that these are just examples, and an algorithm to determine boom “bandwidth” has not been determined. But it also shows that calculation of sonic boom metrics – particularly for low-amplitude booms with long rise times – without consideration for spectral bandwidth may artificially increase the metric levels. Standardization of boom calculations based on effective measurement bandwidth must be considered, particularly when developing protocols for quiet supersonic aircraft certification measurements and data analysis.

5.6.6. Impact of Microphone Configuration on Mean Relative Metrics

At BYU-alpha and BYU-1, there was a comparison between Ground-Board, Elevated, and COUGAR microphone configurations. Channels 4 (Ground-Board) and 5 (Elevated) in Table 5-11 and Channels 3 (Ground-Board) and 5 (Elevated) in Table 5-13 show the acoustical performance of Ground-Board and Elevated relative to COUGAR. COUGAR is shown to be quite acoustically similar to the Ground-Board setup, which is a key outcome of this work: similar high-fidelity acoustical recordings but improved weather robustness. However, the metrics for the Elevated setup at both locations are shown to be consistently lower than for the COUGAR setup, by about 0.8 dB, when one averages across locations and metrics. Although averaging across metrics could be considered somewhat suspect because of their varied

weightings of frequency and amplitude, it is done to illustrate the approximate effect the Elevated microphone has for this setup and boom angle of incidence. Examination of the mean relative one-third octave spectra for the booms for both locations (see Figures 5-15 and *5-16*) shows that there is a notch in the relative spectrum at approximately 800 Hz for the Elevated configuration measurements. The laboratory tests in Section 4 show that this notch is due to the height of the microphone. For the shallow angle of incidence and grassy surface, the Elevated microphone can reduce the sonic boom metrics by more than 1 dB. For greater angles of incidence and a harder ground surface, the interference null will shift to lower frequencies and be greater in magnitude, which would also impact the calculated metric values. This hypothesis is confirmed as part of the CarpetDIEM analysis in Section 6.4.2.

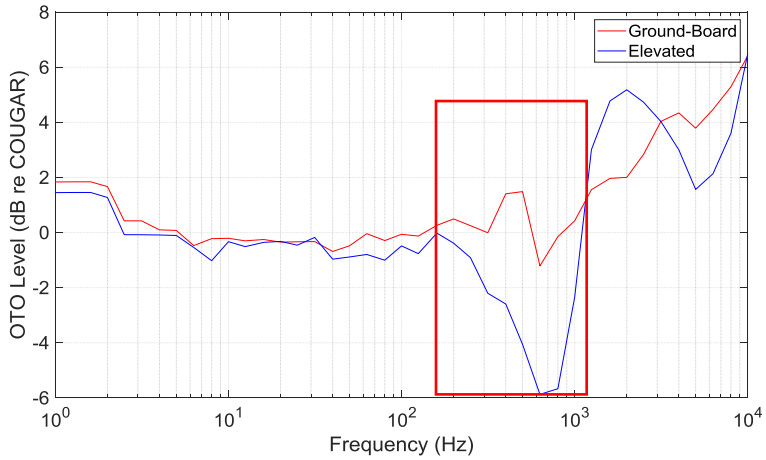

Figure 5-15. Comparison of Ground-Board and Elevated mean relative one-third octave spectra (re: COUGAR) for Booms 18-34 at BYU-alpha. The red box outlines the region around the ground interference null.

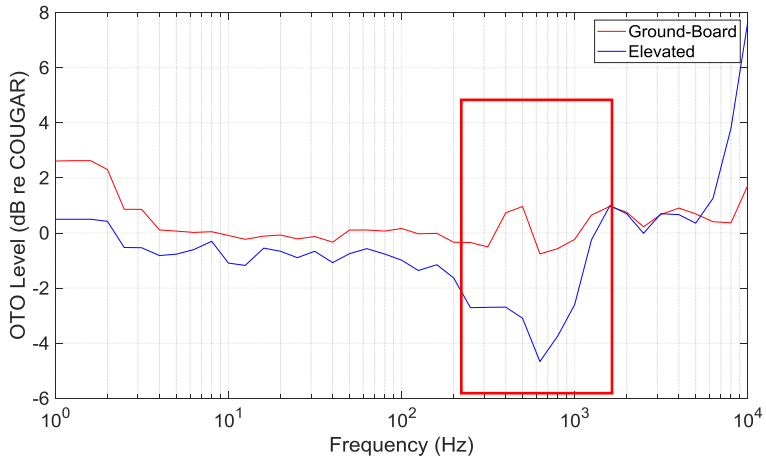

Figure 5-16*. Comparison of Ground-Board and Elevated mean relative one-third octave spectra (re: COUGAR) for Booms 18-34 at BYU-1.*

5.7. Measurement Bandwidth Enhancement

This section describes efforts taken, in collaboration with Dr. Tom Gabrielson of Penn State, to increase the bandwidth using post-processing techniques. A digital pole-shifting filter[x] was used to resolve low-

frequency content outside the flat-response regions of the microphone and data acquisition module and the characteristics of the resulting filters were studied.

5.7.1. Objective

Prior to the QSF18 measurements, laboratory and field tests in Sections 4.4.2 and 4.4.3 showed that low-frequency-capable channels that accurately reproduced waveform shapes also had greater noise above 1 kHz than the other measurement configurations. At present, there is no single hardware choice that fully reproduces the waveform shape and has low noise. This section describes efforts taken to increase the low-frequency bandwidth of low-noise channels using post-processing techniques. The objective is to allow for accurate waveform shape reproduction using high-sensitivity/low-noise measurement configurations. Using individual booms, pole-shifting filter characteristics are determined, investigated, and discussed.

5.7.2. Measurement summary

Each BYU recording station at QSF18 deployed an NI 9250 DAQ module with a GRAS 40AE microphone as well as an NI 9232 DAQ module with a PCB 378A07 sonic boom/infrasound microphone. The former configuration has lower self-noise but has a ~2.4 Hz (-3 dB) low-frequency roll-off for the microphone and 0.43 Hz for the module. The latter configuration has a higher noise floor, but 0.10 Hz roll-off for both microphone and DAQ module. By employing two pole-shifting filters – one for the module and the other for the microphone – the low-frequency response of the NI 9250/GRAS 40AE combination can be extended to match the low-frequency response of the NI 9232/PCB 378A07 combination.

5.7.3. Pole-shifting Filters

The low-frequency roll-off of a microphone is dependent on the characteristics such as input resistance of the preamplifier, pressure-equalization leak, and the built-in DC bias resistor. This limitation affects the shape of the sonic boom waveform and is seen as curvature in the downward slope of the N-wave and a subsequent offset towards positive pressures in the tail shock. Figure 5-17 shows this effect. This waveform distortion makes it difficult for modelers to separate measurement artifact from physical phenomenon, like the impact of turbulence. For quiet supersonic aircraft that produce low-amplitude booms with large rise times, an insufficient low-frequency response also artificially reduces the peak pressure on the bow shock. Note that data acquisition module AC-coupling filters also create their own distortion, but for the DAQ modules used in this test, their -3 dB roll-offs are 0.5 Hz and lower and so the effects are less severe than the microphones. Nonetheless, their responses can be shifted using an additional pole-shifting filter.

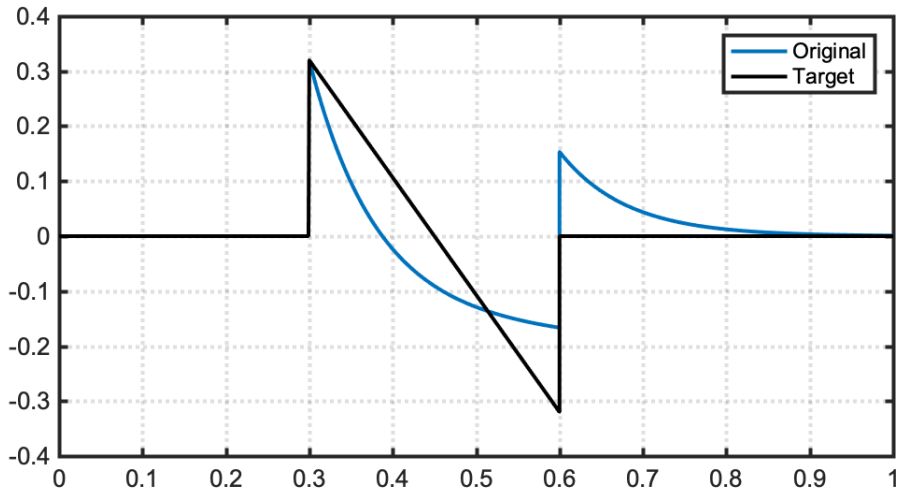

Figure 5-17. A waveform ("Original") showing the simulated effect of the low-frequency response limitation for a microphone. The target N-wave is significantly distorted.

A pole-shifting filter relocates the microphone's cutoff frequency. This frequency appears as a pole in the frequency response. The filter shifts the pole to a more ideal frequency to extend the flat low-frequency response of the microphone while maintaining filter stability in the low-frequency regime. Figure 5-18 shows manufacturer-specified low-frequency responses for the two microphones deployed during QSF18: a PCB 378A07 sonic boom microphone (black line), and a GRAS 40AE free-field microphone (blue). The microphone has a 3 dB-down point around 0.10 Hz, while the GRAS microphone drops below 3 dB at 2.40 Hz. The 0.1-Hz cutoff is assumed to be sufficient to reproduce a sonic boom's waveform shape.

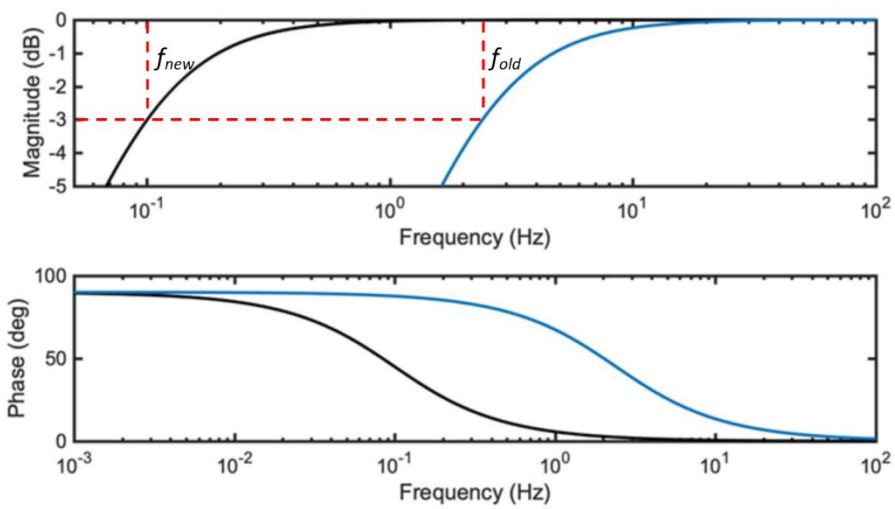

Figure 5-18 Effects of a pole-shifting filter on the magnitude and phase of the microphone's frequency response. The flat response of the microphone is extended to a lower frequency for both magnitude and phase. The black line represents a PCB 378A07 sonic boom microphone, while the blue represents the response of a GRAS 40AE free-field microphone.

The pole-shift filter is the transfer function *H* between the two responses, where f_{old} and f_{new} are labeled in Figure 5-18:

$$H(f) = \frac{f_{old} + j\,f}{f_{new} + j\,f},$$

Figure 5-19 shows the magnitude and phase response of the pole-shifting filter for $f_{old} = 2.4$ Hz and $f_{new} = 0.1$ Hz. At low frequencies, the magnitude approaches a constant gain. This constant gain ensures stability, whereas simply inverting the response of the 40AE microphone would lead to significant noise at low frequencies, particularly due to sources like wind. The phase shifts in the region between the two roll-off frequencies, f_{old} and f_{new}, also approaches zero, as opposed to an increasing gain. Each individual boom at the four BYU QSF18 stations was used to develop pole-shifting filters for both the microphone and data acquisition module through an optimization process. The digital pole-shifting filters are then applied in series.

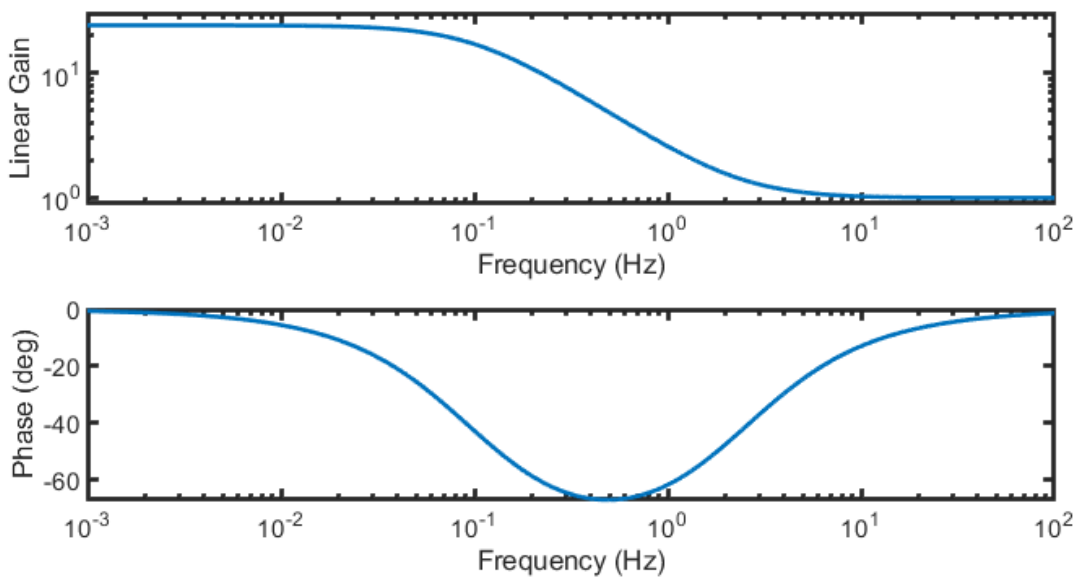

Figure 5-19. Frequency response of the pole-shifting filter. Magnitude slope approaches flat gain at low frequencies.

5.7.4. Filter Optimization

An optimization process is used to find the best parameter fits for the cascaded pole-shifting filters representing the microphone and module responses. There are two parameters for each of the two filters, f_{old} and f_{new}, resulting in a total of four parameters. The process is as follows:

- Fit a quadratic curve to the background noise, and subtract it from the boom waveform, and then subtract the mean value from the resulting waveform.
- Design bilinear pole-shift filters for a pair of cutoff frequencies.
- Filter the measured NI 9250/GRAS 40AE waveform.
- Calculate the mean-square error between the 40AE and the reference waveform measured with the NI 9232/PCB 378A07 microphone and normalize by dividing by the norm of the reference waveform as a function of filter characteristics.

Repeating this process for all boom recordings across the four stations produces a set of possible optimized pole-shifting filters. Each of these filters is then applied to all booms, and the errors again quantified. By doing this, the best possible filter set can be found.

5.7.5. Results

Figure 5-20 shows an example of one waveform with an optimized (minimized normalized mean-square error) filter applied. For all three cases, the low-frequency ambient noise caused by wind has been subtracted from the waveform. The pole-shift-filtered waveform better matches the target waveform as measured by the NI 9232 module and PCB 378A07 microphone. In particular, the linear ramp portion of the waveform has been recovered, and the tail shock portion of the N-wave has the proper amplitude. For the DAQ module pole shift, $f_{old} = 0.80$ Hz and $f_{new} = 0.10$ Hz. For the microphone, its shift is from f_{old} =1.02 Hz to f_{new}= 0.10 Hz. The normalized mean-square difference error of the filtered waveform is ~3 orders of magnitude less than that for the unfiltered waveform.

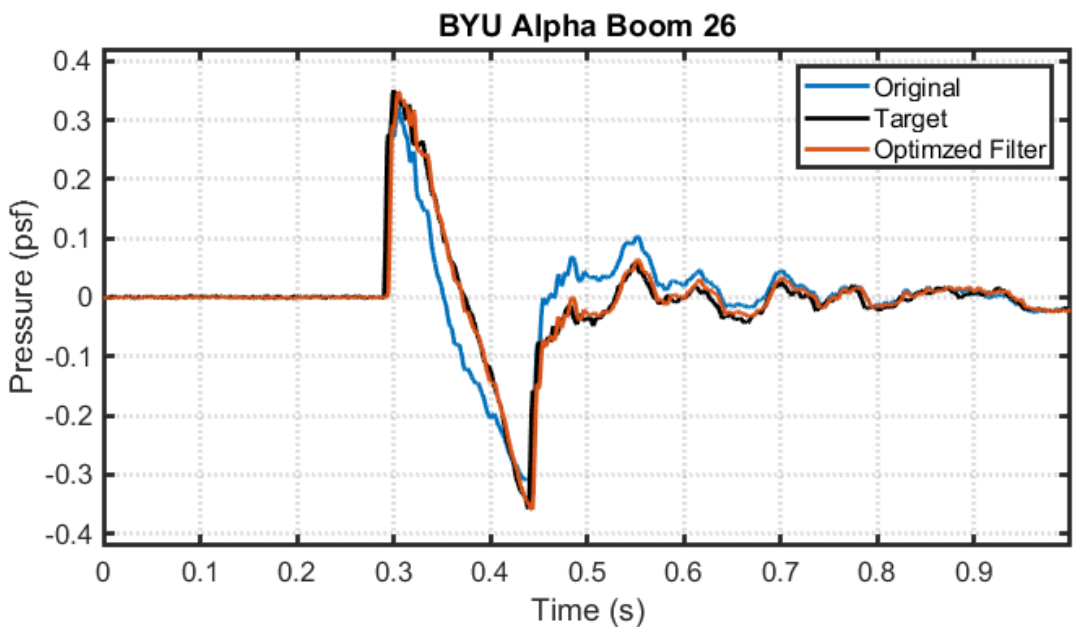

Figure 5-20. Effects of an optimized pole-shifting filter on a single boom.

Applying this same filter across all booms yielded similarly accurate results, as highlighted in Figure 5-21 for four examples. Across all booms and waveforms, applying this filter (derived for one boom and station) resulted in a normalized mean-square error that was at least two orders of magnitude less than that of the unfiltered waveform.

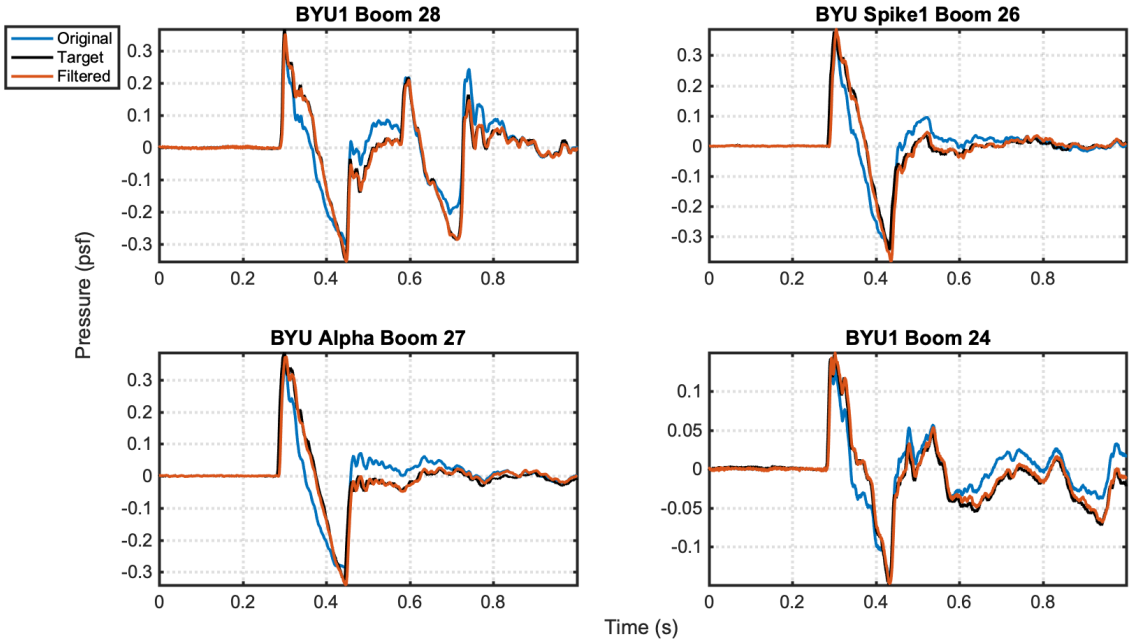

Figure 5-21. The pole-shifting filter process applied to various booms.

Although the pole-shifting filter approach above has been shown to be successful, it requires two microphone systems. By using manufacturer specifications, it is possible to use a single microphone system and achieve similar results with slightly lower accuracy. As a comparison with the optimized filtering approach, a filter built from the specifications sheet, denoted as a 'Manufacturer Specs Filter,' was also applied to each boom. For QSF18 measurements, this equates to a module filter of $f_{old} = 0.43$ Hz (NI 9250) to $f_{new} = 0.10$ Hz (NI 9232), and a microphone filter of $f_{old} = 2.4$ Hz (GRAS 40AE) to $f_{new} = 0.10$ Hz (PCB 378A07). A time-waveform comparison can be seen in Figure 5-22. This filter was not as effective as the individual boom-and-station-optimized filter, as it overcompensates for the low-frequency response loss. This assumes that the low-frequency combination represents the current most physically accurate measurement available. In considering these results, it is possible that manufacturer specifications are a conservative estimate of the low-frequency response, i.e. the manufacturer specifications for low-frequency cutoff are given as a worst-case scenario for a particular microphone model. Preliminary investigations suggest that, when using the manufacturer-specified cutoff for the DAQ module, a manufacturer-specified microphone filter designed around $f_{old} = 1.7$-2.0 Hz may be more accurate. However, this is left for future work.

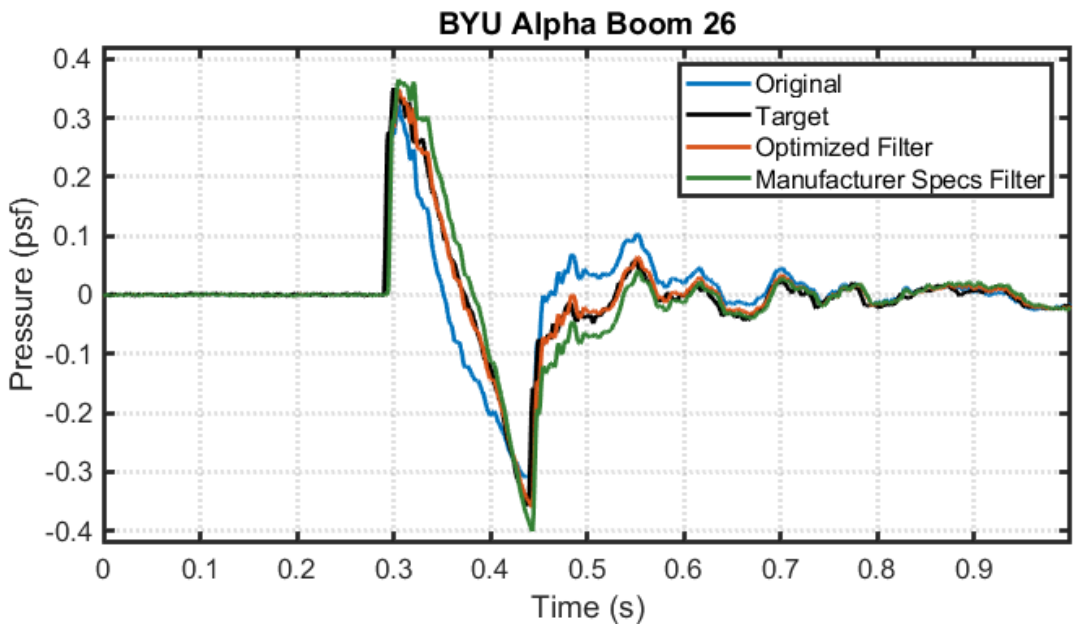

Figure 5-22. Comparison of an optimized filter to a filter created with manufacturer specifications.

The goal of the pole-shifting is to improve the waveform shape's physicality by enhancing the low-frequency response of the measurement system. The low-frequency spectral content of the filtered waveform is boosted several decibels, based on the gain of the filter. An example is shown in Figure 5-23. The primary result of this analysis is that the pole-shift filtered system matches the target low-frequency response without a high noise floor above 1 kHz. Both of these approaches highlight the usefulness of the pole-shifting filter at improving the low-frequency response of sonic boom measurements using conventional measurement configurations. The manufacture specification filter tended to overestimate the low frequency content of the signal in this case.

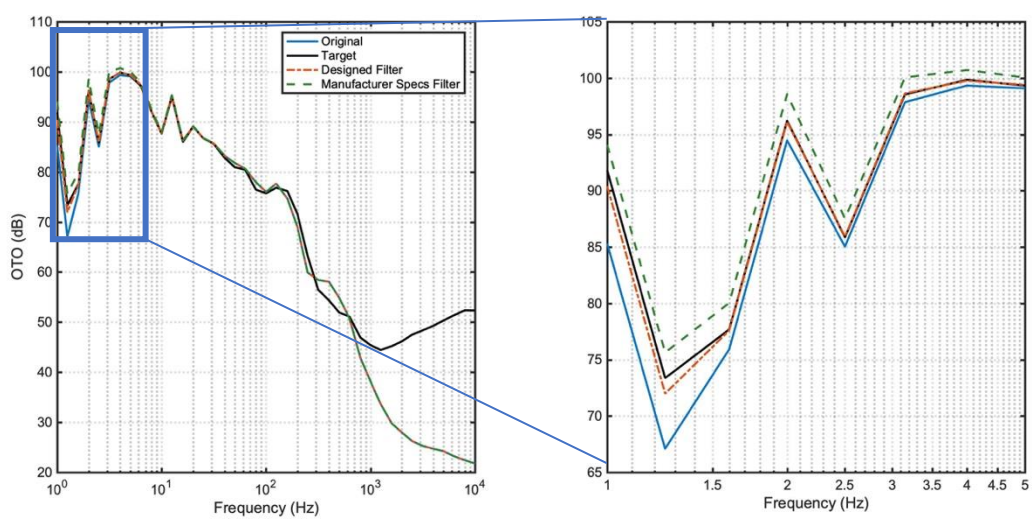

Figure 5-23. One-third octave spectrum from a single boom, calculated with 1 second of data. Left: Spectrum up to 10 kHz. Right: Enlarged portion of spectrum up to 5 Hz. Filtered waveforms better match target low-frequency response while maintaining a lower noise floor at high frequencies.

5.7.6. Impact on Metrics

Applying the filters does not appreciably impact metrics being considered for assessing human response to sonic booms. The average effect of the pole shifting is approximately 0.1 dB. However, for the Z-weighted SEL, pole-shifting the NI 9250/GRAS 40AE channel to the target channel's characteristics results in a low-frequency boost with average increase of 0.8 dB.

5.7.7. Filter Robustness

Averaging across all booms and stations results in the following optimized mean filter characteristics: the data acquisition module filter shifts the cutoff from $f_{old} = 0.46 \pm 0.29$ Hz to $f_{new} = 0.10 \pm 0$ Hz, and the microphone filter shifts the cutoff from $f_{old} = 1.07 \pm 0.35$ Hz to $f_{new} = 0.15 \pm 0.05$ Hz. The original pole has higher deviation, most likely due to variance within the microphones themselves. Averaged over four sets of microphones and many booms, these results represent the optimal QSF18 pole-shifting filter design. For a given station, it is best to optimize a filter with two microphones, one low noise combination and one quality low-frequency combination if available, for a given set of measurements. However, it is still acceptable to use either a previously optimized filter or a filter based on the manufacturer specifications for a low noise floor measurement system.

In order to test the applicable range of the QSF18 optimized filter, the filter was applied to a sonic boom created from the Falcon 9 stage-1 reentry described in Section 4.4.3. As seen in Figure 5-24, this is a markedly different sonic boom from the QSF18 quiet booms, with its characteristic triple-boom shape, sharper shocks, and longer duration. Unfortunately, the measurement of the front shock for the "original" waveform was clipped. Despite the clipped measurement, the pole-shifted waveforms, whether from QSF18 or the manufacturer, greatly improved the sonic boom shape relative to the original. All filters reduced the normalized mean-square error by two or more orders of magnitude.

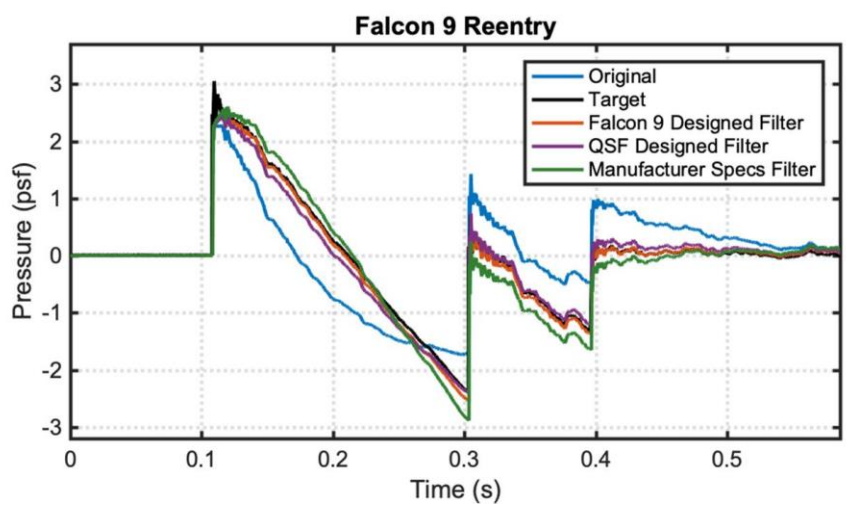

Figure 5-24. Comparison of filters applied to a sonic boom created from a Falcon 9 stage-1 reentry.

While an optimized filter is better on a test-by-test basis, a manufacturer or previously designed filter can be also used. The pole-shift filter improves the low-frequency response, as well as recovers shape characteristics in the time domain. Further investigations can be made into filtering steady-state noises, or other types of sonic booms. It is expected that pole-shifting filters can improve low noise measurements in situations where low-frequency information is limited.

6. CarpetDIEM Test Campaign

6.1. Objectives

The Carpet Determination In Entirety Measurements (CarpetDIEM) test campaign seeks to develop and test a linear array of high-fidelity measurement stations in preparation for low-boom flight qualification of the X-59. BYU participated in this test campaign during Summer 2019. BYU's objectives for this campaign were the following:

- Field a total of eleven time-synced stations across approximately 10 nautical miles (NM) to help study boom carpet width
- Learn important logistics regarding testing in this region, which is proposed for initial X-59 testing
- Test improved PUMA data acquisition capability
- Verify some conclusions of the QSF18 tests regarding microphone types and configurations, in a cleaner measurement environment and for regular cruise booms
- Field-test the next iteration of the COUGAR: the COUGARxt
- Examine sonic boom variability over short distances and investigate the relevance of local measurement arrays for understanding measurement uncertainty

6.2. Station Design

The stations deployed by BYU were designed to be rapidly deployable, weather robust, and capable of high-fidelity sonic boom measurement. PUMA and COUGAR (as outlined in Section 4) were the basis of each station deployed by BYU. The configurations of these stations, organized by a number assigned to each PUMA, are demonstrated in

Table 6-1.

For continuity, ten equipped PUMA systems were outfitted with a base configuration of an NI 9250 low-noise input module and a GRAS 47AC low-frequency response microphone in a COUGAR microphone setup. Relative to QSF18, this microphone has a slightly improved low-frequency response, larger dynamic range, and greater sensitivity than the PCB 378A07. Some microphones were also used as part of the 27 microphones employed. All stations were equipped with a GPS time clock for time synchronizing the recordings across stations for analysis, as well as the Kestrel meteorological instrumentation.

Table 6-1. Summary of BYU PUMA Configurations for CarpetDIEM.

PUMA #	# Microphones	Configuration
1	4	**COUGAR Base Configuration**
		COUGAR/Ground-Board/Elevated Comparison
2	7	**Linear Microphone Array**
3	4	**COUGAR Base Configuration**
		COUGAR/Ground-Board/Elevated Comparison
4	1	**COUGAR Base Configuration**
5	1	**COUGAR Base Configuration**
6	3	**COUGAR Base Configuration**
		COUGAR/COUGARxt Comparison
7	1	**COUGAR Base Configuration**
8	3	**COUGAR Base Configuration**
		COUGAR/COUGARxt Comparison
9	1	**COUGAR Base Configuration**
10	1	**COUGAR Base Configuration**
11	1	**COUGAR Base Configuration**

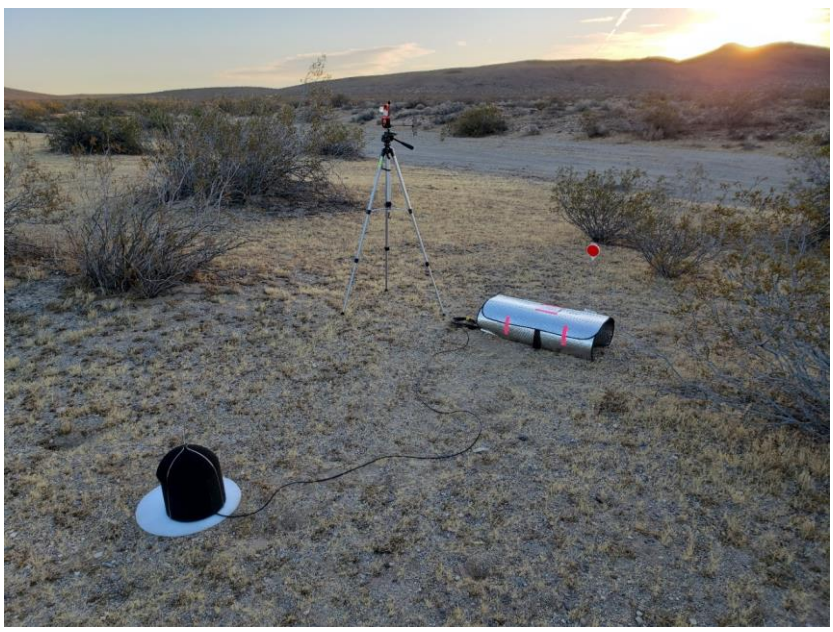

Figure 6-1. Basic site configuration with a single microphone, data acquisition system in sun shield and weather instrumentation.

In addition to the basic configuration, four of the ten comparison sites were also outfitted with configuration comparisons, including comparisons between COUGAR, Elevated, and Ground-Board microphone configurations (see Figure 5-2) and a comparison of the revised and improved COUGARxt configuration with the original COUGAR.

Due to the heat experienced during late morning and early afternoon tests, PUMA cases were stocked with dry ice blocks in addition to cooling fans to ensure that the data acquisition computers did not overheat. This cooling solution had a duration of approximately 4 hours without resupply. The outsides of PUMA cases were also covered with a reflective sun shield to further reduce the heat transmission to the inside of the PUMA case. This method proved to be effective in keeping the system from overheating with ambient temperatures in excess of 38°C (100°F).

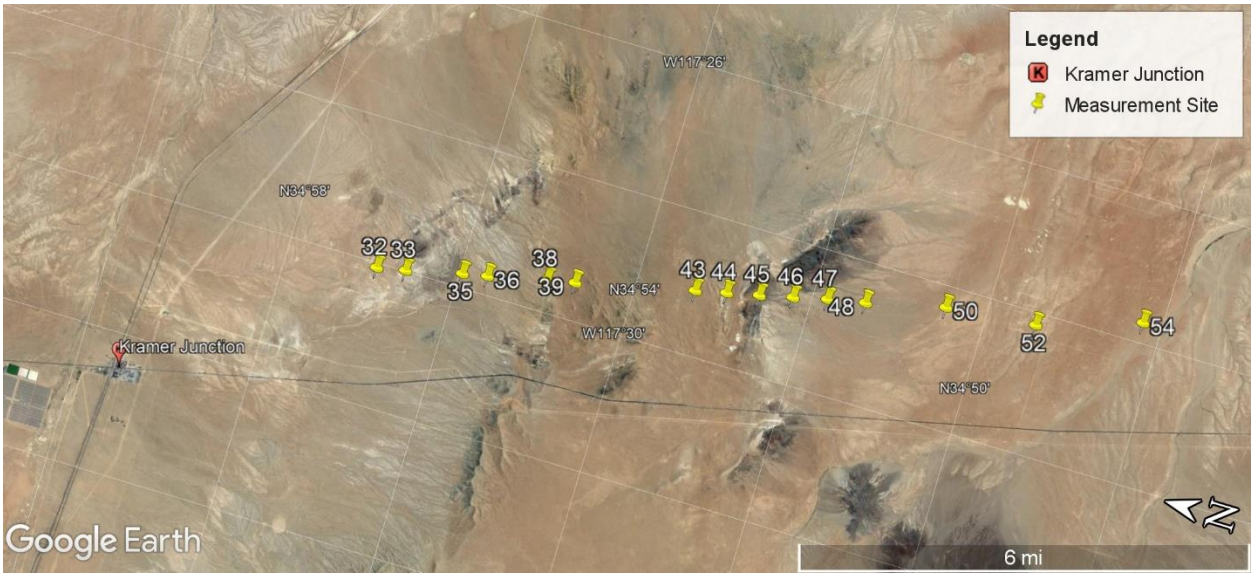

Figure 6-2. BYU Array Stations. The span of the array is approximately 10 NM.

6.3. Summary of Booms Recorded

Twenty-three booms were measured during the test campaign. A summary of the booms recorded is presented in Table 6-2. Successful boom recordings are noted by a peak pressure (in PSF). Unsuccessful recordings are noted by highlighted cells; red with “HE” representing a hardware error resulting in no data, red with “TE” representing a triggering error resulting in no data, and yellow with “SE” representing a storage error where recorded data disappeared off of the encrypted storage device.

Table 6-2. Summary of booms recorded across stations. Peak pressures for booms recorded in PSF. Cells highlighted in red with "HE" represent a hardware error resulting in no data. Cells highlighted in red with "TE" triggering error resulting in no data. Cells highlighted in yellow with "SE" represent a storage error where recorded data disappeared off of the storage device.

		PUMA										
		1	2	3	4	5	6	7	8	9	10	11
Boom	1	1.97	1.87	1.37	1.62	1.60	0.97	0.85	HE	0.62	0.98	SE
	2	1.88	1.67	1.34	1.12	1.73	1.13	1.53	HE	0.31	0.70	SE
	3	1.60	1.43	1.35	1.30	TE	1.01	0.92	HE	0.36	0.93	SE
	4	1.83	1.34	1.34	1.55	TE	0.85	0.86	HE	0.50	0.74	SE
	5	1.90	1.68	1.34	2.03	1.08	0.93	1.45	1.50	0.56	3.01	SE
	6	2.28	1.37	2.15	1.47	1.63	1.20	2.18	1.60	0.73	1.94	SE
	7	2.10	2.65	1.12	1.72	1.77	1.58	1.35	1.00	0.97	1.68	SE
	8	2.27	3.31	2.04	1.30	1.54	2.82	2.56	0.66	0.73	0.89	SE
	9	1.51	1.55	1.85	1.71	1.39	1.68	1.89	1.52	1.16	0.99	1.62
	10	1.80	2.03	1.54	2.23	1.44	1.56	1.74	0.82	0.86	0.69	1.69
	11	1.65	1.29	2.04	1.05	1.51	1.36	1.58	1.37	1.24	0.68	1.39
	12	1.39	1.88	1.78	1.76	1.54	1.51	1.17	3.61	0.88	1.29	1.65
	13	1.55	3.09	1.56	1.25	1.19	1.83	1.27	1.33	1.88	0.96	2.25
	14	1.42	1.57	1.79	4.50	TE	1.34	0.99	2.55	1.27	0.66	1.52
	15	1.69	3.10	2.94	1.28	TE	1.54	1.99	1.24	1.63	1.24	1.50
	16	1.61	4.70	2.00	2.46	TE	1.72	1.99	1.54	1.02	0.53	2.47
	17	1.95	1.89	1.66	1.24	1.44	0.97	1.33	1.14	1.20	0.22	2.02
	18	1.77	2.29	1.45	1.30	1.18	1.38	1.04	1.70	0.89	0.66	1.83
	19	1.60	3.30	1.51	1.88	1.55	0.93	0.97	1.11	0.92	0.40	2.37
	20	1.26	1.06	1.01	1.24	1.53	1.25	1.36	SE	2.14	0.87	1.52
	21	1.57	1.37	1.08	0.78	0.92	0.90	0.81	SE	0.79	0.57	1.51
	22	1.57	1.31	1.83	1.70	1.06	0.86	2.94	SE	1.00	0.73	1.45
	23	1.70	1.91	1.54	1.71	1.93	2.53	1.42	SE	0.99	0.54	1.79

All three triggering capabilities outlined in Section 4.2.1.2 were employed at CarpetDIEM. Every method proved to be reliable, and only five triggering error incidents were identified. This resulted in a triggering performance of 248/253 recordings (98%).

6.4. Data Analysis

Data analysis is limited under this program scope, but data were validated across stations to provide a preliminary overview of BYU array performance. Base configurations across ten stations allows for a comparison of booms across a large-scale array of 10 nautical miles (NM). The impact of microphone configuration is examined to validate findings from the QSF18 campaign. The wind noise rejection of COUGARxt is compared to COUGAR. Additionally, the linear microphone array is characterized for a limited number of booms, with perceived levels, spectra, and waveforms, to demonstrate the viability and need for this kind of an array.

6.4.1. Example Results across All Stations

Figure 6-3 shows the recorded waveforms across all BYU stations for Boom 11. Arranged according to site number, the center of the flight path was nominally at station 36. Differences in waveform shape and

amplitude are apparent across stations, with a noticeable attenuation towards the southern edge of the array (labeled as sites 47-54). Further investigation into meteorological and terrain conditions may yield information on the variations in waveforms across the array. However, one important point is noted: site 54, which was the south end of the array, recorded all booms. Thus, the true width of the boom carpet was not determined at the southern end of the array. The NASA SPIKE sensors deployed on the northern portion of the array were able to determine the half-width of the carpet for some passes.

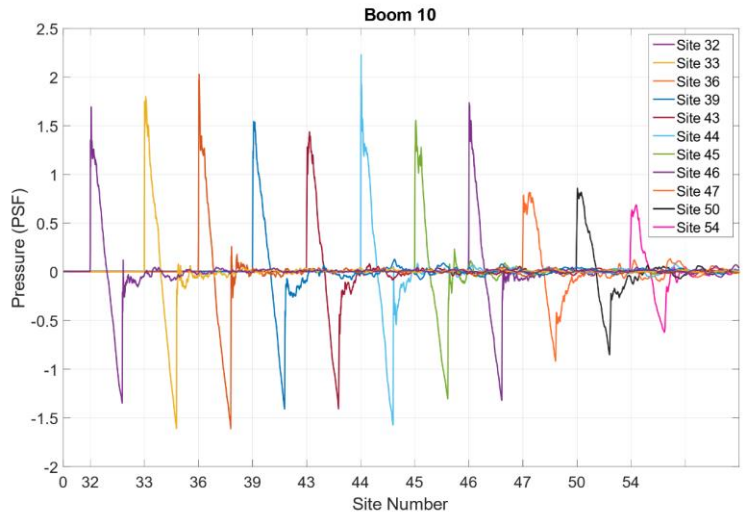

Figure 6-3. Example of Boom 10 across all 11 BYU array stations. Noticeable attenuation can be observed towards the peripheries of the array (stations 47-54) while variation in bow shock amplitude is substantial across sites closer to the flight path center.

Bow shock arrival times across the array are observed to be the corollary that relates to the distance from the center of the flight path. Figure 6-4 shows the arrival time of booms across the BYU stations for Boom 10, relative to the center of the array. These arrival times qualitatively fit what would be expected with the hyperbolic shape of the boom carpet, but suggest that the effective center of the array for this case is somewhere between sites 33 and 36. Future quantitative analysis is merited, given that factors such as aircraft speed, altitude, trajectory and meteorological conditions may affect the arrival times of the booms.

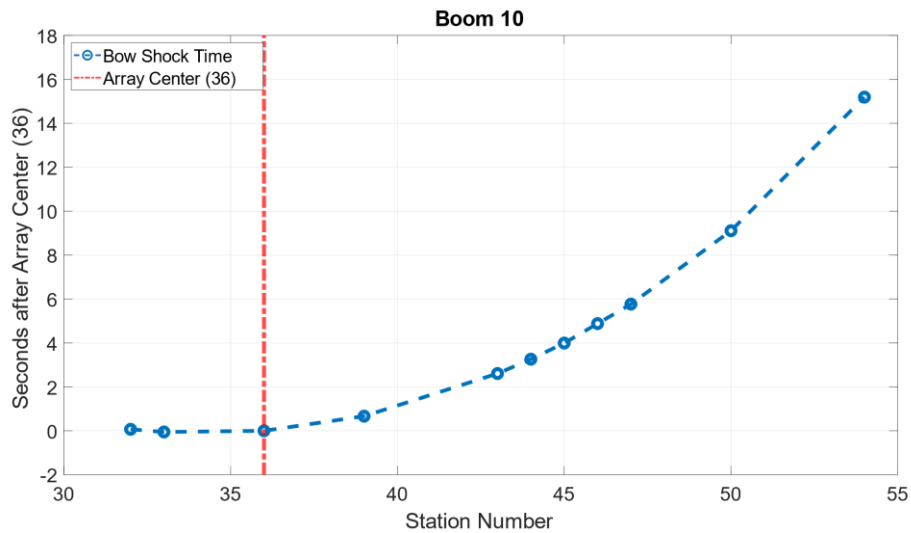

Figure 6-4. Arrival times of Boom 11 relative to center station at site 36.

6.4.2. Microphone Configurations

Microphone configuration comparisons were made at four different sites during the test campaign. Two stations evaluated the performance of COUGAR, Ground-Board and Elevated microphone configurations, while the two other locations evaluated COUGAR and COUGARxt configurations. A report of the latter comparisons is given in Section 6.4.3.

Figure 6-5. Microphone configuration comparison site at PUMA 1. Clockwise from top: COUGAR, Ground-Board, Elevated, COUGAR.

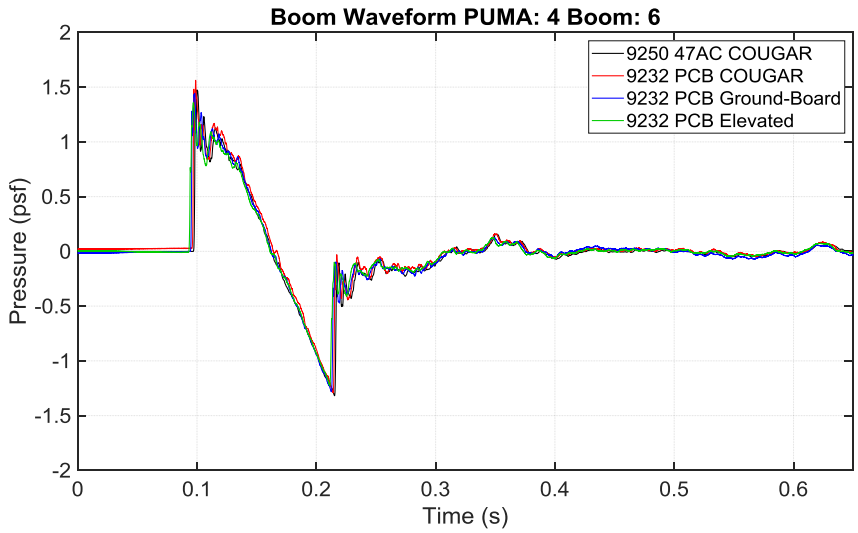

Figure 6-6. Boom 6 Waveform at Site 44. Average Windspeed of 4.6 m/s (10 mph).

Spectral comparisons demonstrate that setups featuring thicker windscreens and microphones closer to the ground provide the greatest wind noise rejection. Figure 6-7 demonstrates this wind noise rejection between configurations during a period of ambient wind noise with wind speeds approaching 5 m/s. The COUGAR configuration has the lowest amount of wind noise present, followed by the Ground-Board configuration and finally the Elevated configuration with the most wind noise. This result matches prior observations during QSF18.

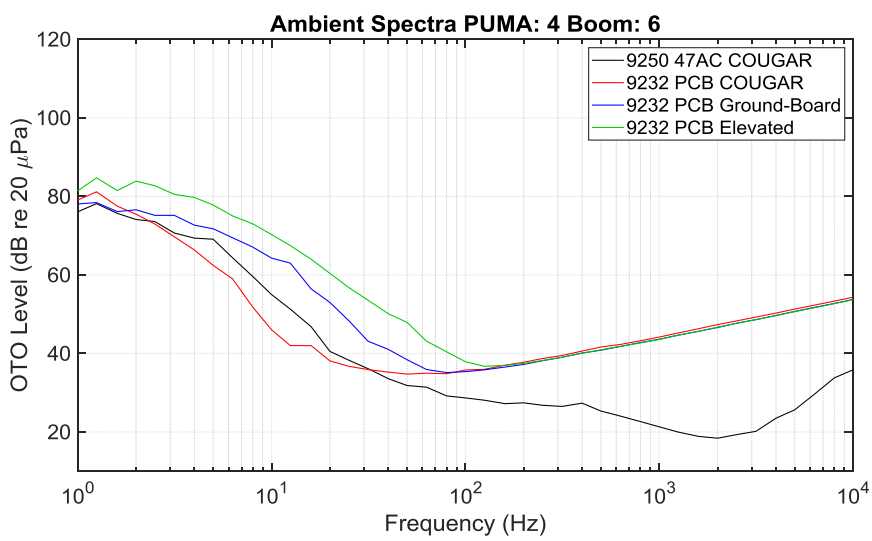

Figure 6-7. Boom 6 ambient spectra at Site 44, where there was an average wind speed of 4.6 m/s (10 mph). The relative wind noise rejection of the different setups is visible among lower frequencies.

Wind noise rejection of configurations has a significant effect on the signal-to-noise ratio (SNR) of the recorded booms. Figure 6-8 displays the one-third octave spectrum of Boom 6 whereas Figure 6-9 shows the one-third octave SNR of Boom 6 relative to the ambient spectra immediately preceding the boom. COUGAR provides the highest SNR especially within the 2-100 Hz range. At 10 Hz, COUGAR provides an additional 10 dB of SNR over the Ground-Board configuration, and 14 dB over the Elevated configuration.

For quiet booms, this added increase in SNR due to wind noise rejection would provide an increased effective measurement bandwidth.

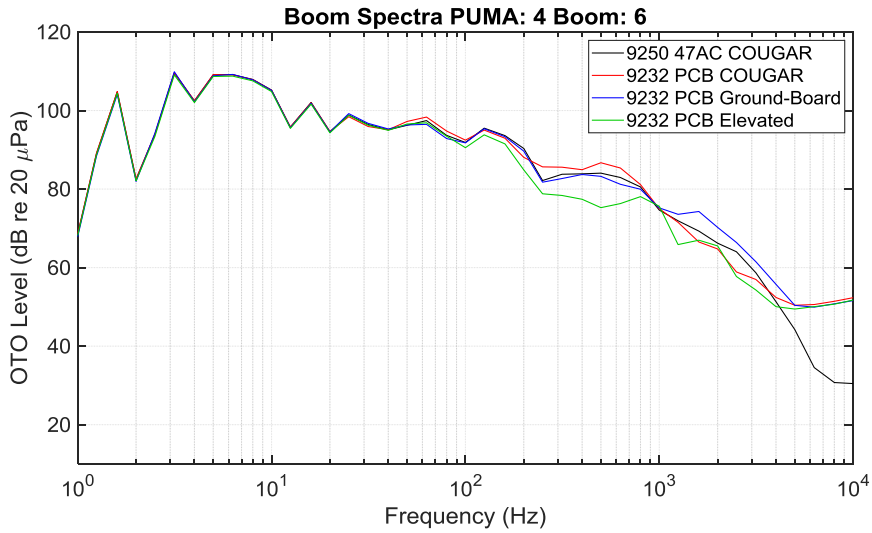

Figure 6-8. Boom 6 one-third octave spectra at Site 44. Average wind speed of 4.6 m/s (10 mph).

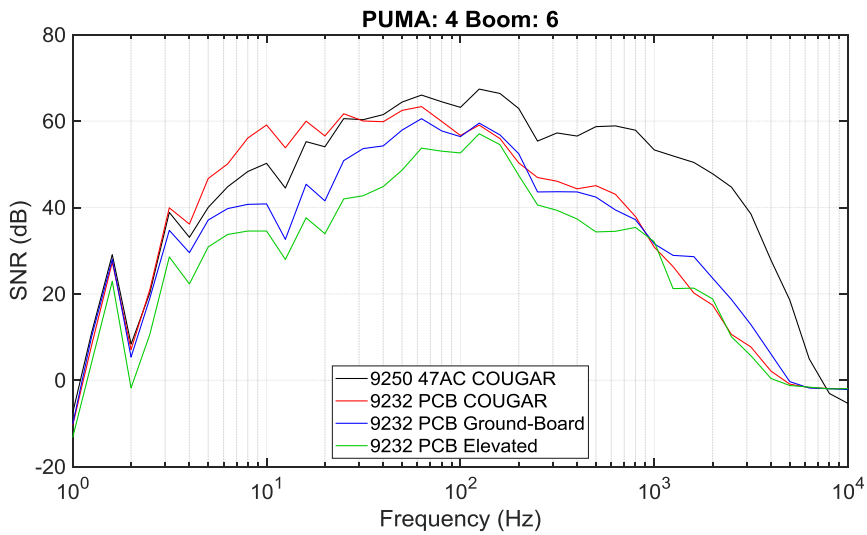

Figure 6-9. Boom 6 signal to noise (ambient) ratio at Site 44. Average wind speed of 4.6 m/s (10 mph).

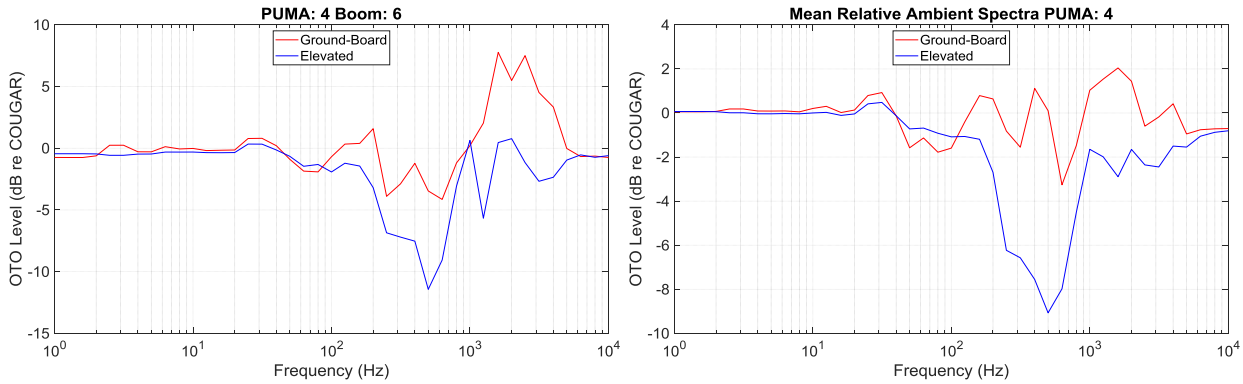

Figure 6-10. Left: Ground-Board and Elevated relative to COUGAR for PUMA 4, Boom 6. The characteristic losses of Elevated between 100 and 1000 Hz are apparent. Right: Mean relative spectra for PUMA 4 relative to COUGAR across all booms.

Another comparison that was revisited as part of CarpetDIEM is the demonstration that Ground-Board and COUGAR are acoustically similar but that the elevation of the microphone in the Elevated setup creates challenges. Figure 6-10 shows one-third octave spectra of Ground-Board and Elevated microphone configurations for PUMA 4, for Boom 6 (left), and averaged over all booms (right). The results demonstrate that Ground-Board behaves acoustically similar to COUGAR (to within $\pm$ 2 dB at all frequencies). However, the Elevated configuration exhibits large losses approaching -8 dB in frequencies between 100 and 1000 Hz. In comparing to the QSF18 results in Figure 5-15 and Figure *5-16*, the nulls are deeper (due to the harder surface), and peak at a slightly lower frequency (due to the angle of incidence being greater relative to grazing).

An analysis of the candidate sonic boom metrics confirms the acoustical similarity between COUGAR setups, between Ground-Board and COUGAR, and also the impact of the Elevated microphone configuration. Table 6-3 shows the mean differences between setups at PUMA 4 relative to one of the two COUGAR setups. In this case, the NI 9232/PCB 378A07 COUGAR setup was chosen as the baseline to provide for maximum consistency with the Ground-Board and Elevated channels – the DAQ channel and microphone type were identical across the three setups. However, the two COUGAR setups were also quite similar. In comparing Ground-Board and COUGAR, all metrics are within 0.2 dB of each other, excepting the B-weighted SEL, which differed by 0.3 dB. However, the underestimation of the metrics by the Elevated setup are worse than for QSF18 (see Table 5-11 and Table 5-13 and surrounding discussion. Instead of 0.5 – 1 dB, some metrics exceed 2 dB, with the greatest difference in the A-weighted SEL of 3.4 dB. In summary, a microphone raised off the ground – by causing an interference null at several hundred hertz – will result in a significant (> 1 dB) underestimation of most sonic boom metrics.

Table 6-3. Mean differences in metrics for PUMA 04 in dB re: NI 9232 COUGAR.

	PL	ZSEL	ASEL	BSEL	CSEL	DSEL	ESEL	ISBAP
NI 9250 47AC COUGAR	-0.5	-0.1	-0.03	-0.2	-0.2	-0.1	-0.1	-0.6
NI 9232 COUGAR	-	-	-	-	-	-	-	-
NI 9232 Ground-Board	**-0.04**	**0.06**	**-0.2**	**-0.3**	**-0.1**	**-0.2**	**-0.2**	**-0.02**
NI 9232 Elevated	**-2.1**	**-0.03**	**-3.4**	**-1.4**	**-0.3**	**-1.3**	**-2.2**	**-0.8**

6.4.3. COUGAR vs. COUGARxt

CarpetDIEM provided a unique opportunity to test COUGAR and COUGARxt. Both were tested at three different stations – 45 (PUMA 6), 47 (PUMA 8), and 48 (PUMA 8). An example of how station 45 was set up is shown in Figure 6-11. The waveforms match very closely between the two configurations, shown in Figure 6-12. In comparing the COUGARxt to COUGAR relative spectra across all booms in Figure 6-13, the one-third octave levels are within ± 1dB up to 1 kHz. Beyond that, noise floor variability prevents meaningful comparison.

Figure 6-11. CarpetDIEM station 45 with three configurations. Two of the configurations are COUGAR; the other, right-most in this figure, is COUGARxt.

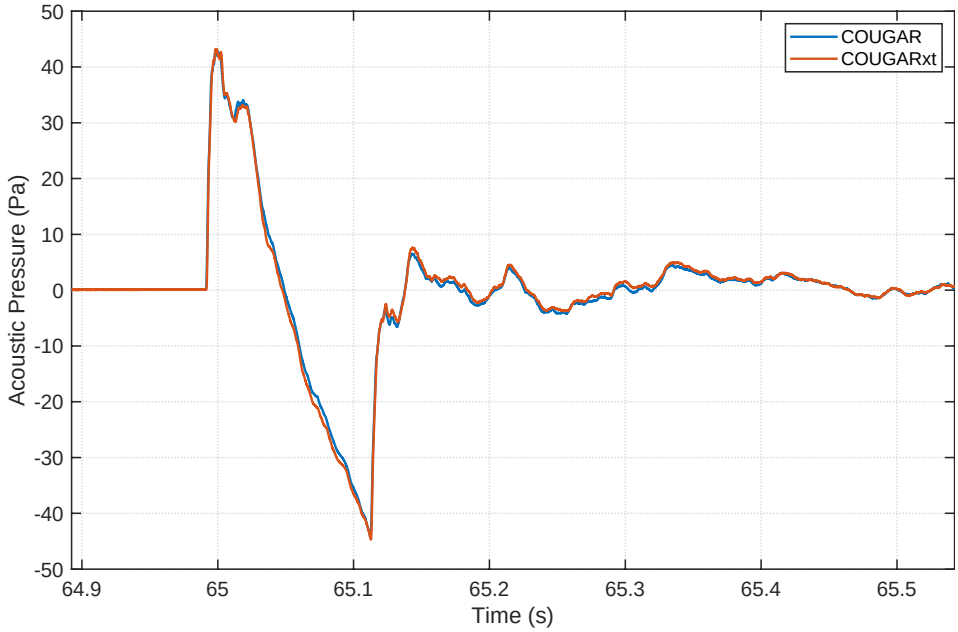

Figure 6-12. Pressure waveform from Boom 1 at station 45. Both configurations used a GRAS 47AC microphone.

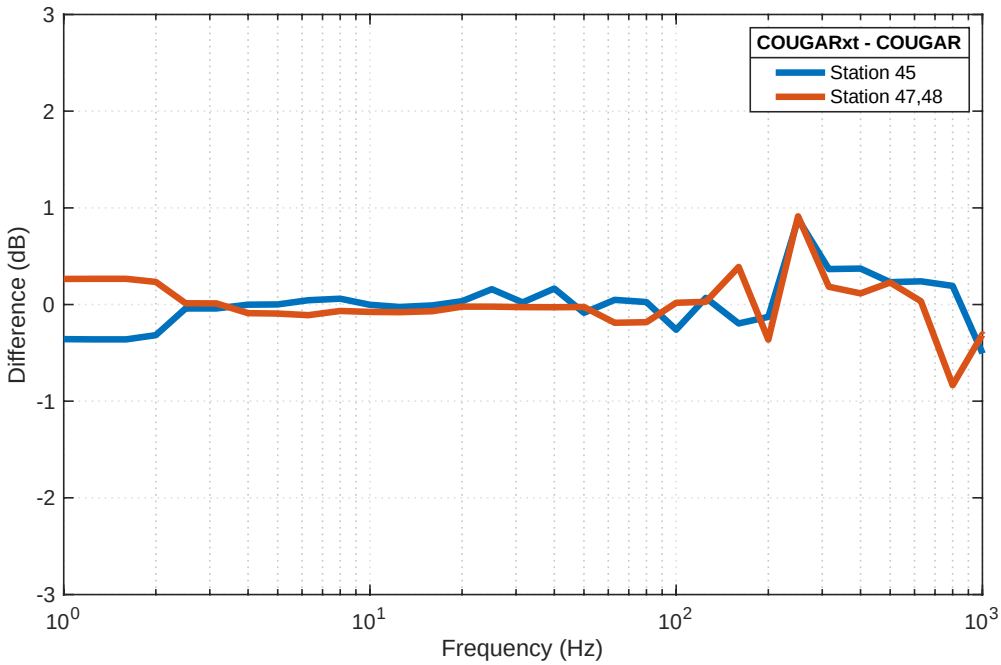

Figure 6-13. Average difference between COUGARxt and COUGAR over all recorded booms at stations 45 (PUMA 6), 47 (PUMA 8) and 48 (PUMA 8). Stations 47 and 48 are paired together because the instrumentation was at station 47 for the first two days and at 48 for the final day. Data are only shown to 1 kHz because several booms ran into the noise floor shortly after 1kHz.

6.4.4. Linear Microphone Array

One notable issue that causes difficulty in developing standardized measurement methods for supersonic aircraft certification and for associated community testing is atmospheric turbulence.[xi] To investigate the possible local variation of sonic boom properties (e.g., due to atmospheric turbulence) in the vicinity of a measurement site at CarpetDIEM, a linear microphone array was deployed at one site at the center of the anticipated flight path (site 36). The linear array consisted of seven microphones, running roughly North to South and perpendicular to the anticipated flight paths of the aircraft, as demonstrated in Figure 6-14. The PUMA was placed near the center microphone, and microphones were located 15 m (50 ft), 30 m (100 ft) and 61 m (200 ft) to the North and South of the center microphone. Due to resource limitations, two different microphone types were utilized in the array: GRAS 40AE microphones at the center and both locations 15 m (50 ft) from the center, with the remaining four microphones at 30 and 61 m (100 and 200 ft) from the center being PCB 378A07 microphones.

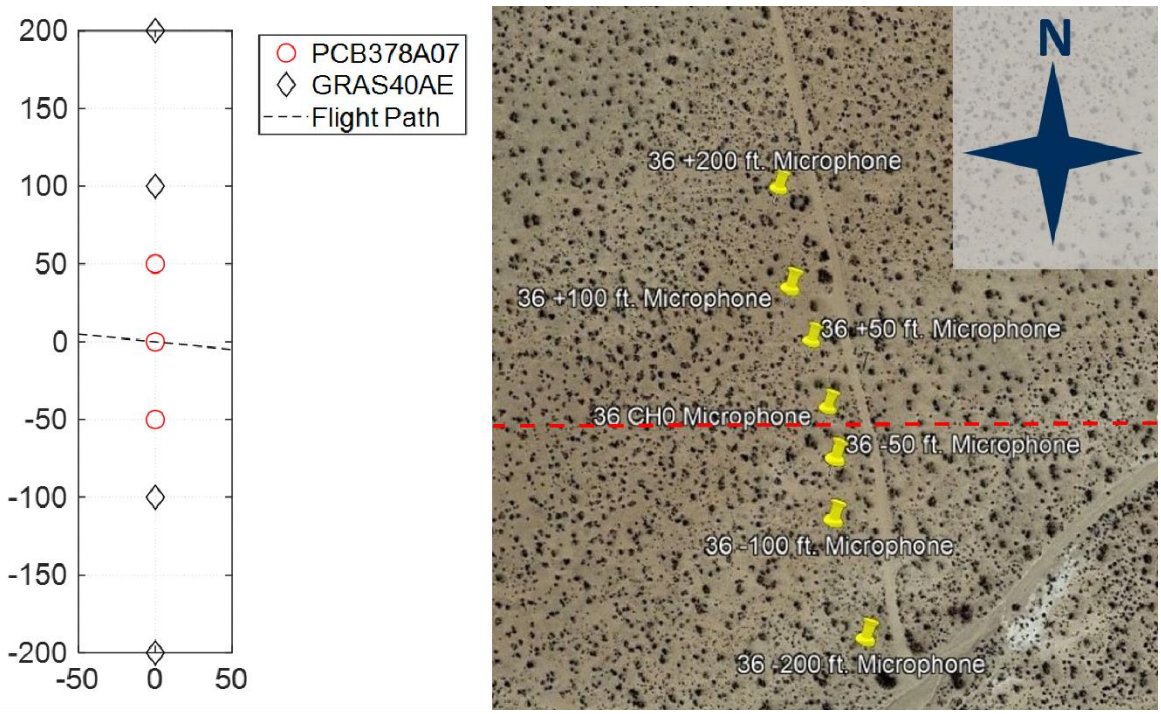

Figure 6-14. Linear microphone array layout (right) with distances in feet. Dashed lines on both figures represent the anticipated center of the flightpath.

Key to the interpretation of array measurements are local meteorological data. These data were measured and recorded by a portable weather station located at the center microphone at a height of 1.5 m (5 ft). The weather station was able to record meteorological data for five out of the six flights. These data include wind speed and direction, barometric pressure, temperature, and humidity. The highest average wind speeds of the test series occurred around Boom 14, with an average wind speed of 3.5 m/s (7.8 mph).

Similar to the Falcon 9 measurements in Section 4.4.3, an issue with microphone type resulted in occasional clipping of the bow shock on some of the highest amplitude booms. The ~50 mV/Pa sensitivities of the GRAS 40AE microphones produced signals exceeding the 5 V maximum input range on the data acquisition hardware when acoustic pressures exceeded ~96-120 Pa (~2-2.5 psf). This should not be an issue for measurement of quiet-boom aircraft.

Differences in recordings across the array are apparent. Arrival times differed slightly between microphones, as expected, although the ordering can be unintuitive. The recorded waveforms also exhibit differences in amplitude, especially in the bow and tail shock areas. Figure 6-15 demonstrates these differences observed in the waveforms for Boom 14. Microphones south of the center microphone [-15, -30, -61 m (-50, -100, -200 ft)]. all exhibit a more peaked bow shock, greater in amplitude than the center and north microphones by approximately 24 Pa (0.5 psf).

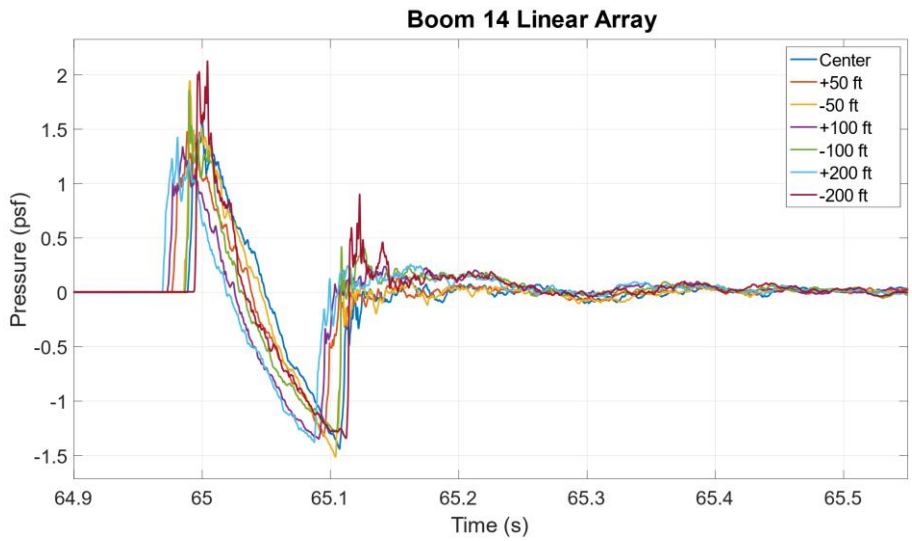

Figure 6-15. Boom 14 recorded at the linear microphone array in an average wind speed of 3.5 m/s.

Spectral variations also are present between boom recordings across the array. Figure 6-16 shows the one-third octave spectra across the array for Boom 14. These variations start at about 10 Hz, presenting an approximate spread of 10 dB across frequencies from 20 to 1000 Hz. Generally, lower frequencies in the infrasound regime ($f < 10$ Hz) are consistent across all microphones.

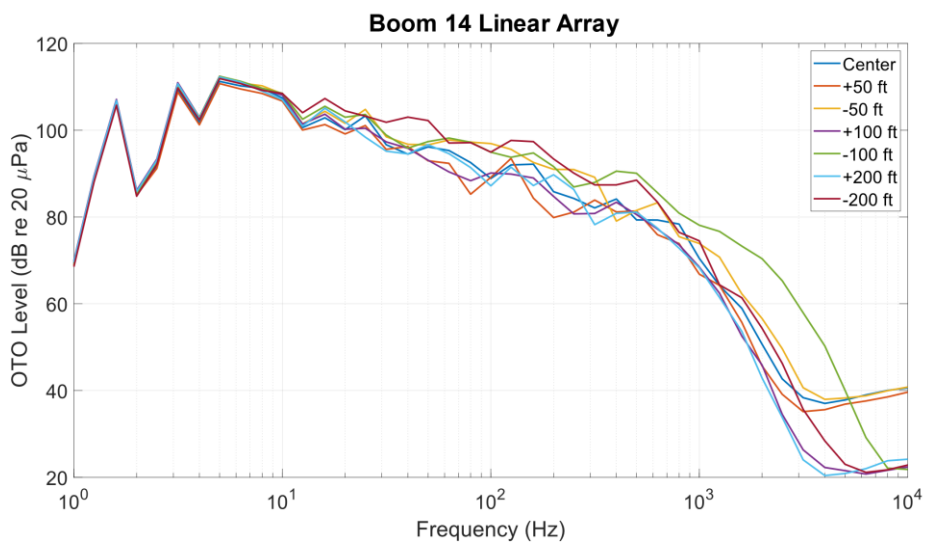

Figure 6-16. One-third octave spectra of Boom 14 recorded across the linear microphone array.

The perceived levels for Booms 4 and 14 are shown in Figure 6-17 and Figure 6-18, respectively. For Boom 14, there is an 8+ dB difference in PL between microphones across the array. For Boom 4, the maximum difference is 11+ dB over 46 m (150 ft). This result indicates a large relative statistical uncertainty in a single measurement at one location. This kind of uncertainty qualitatively matches the kinds of spatial variation seen by Stout and Sparrow. [xii,xiii]

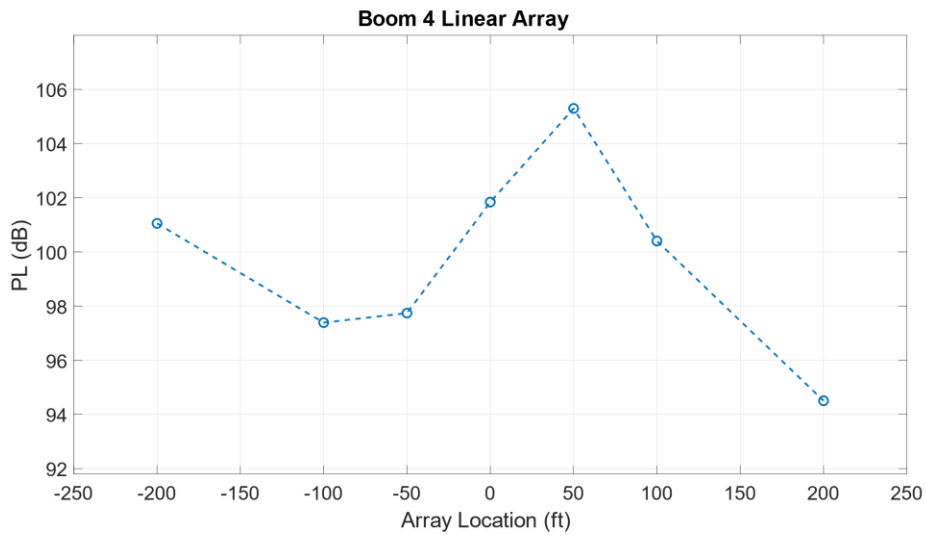

Figure 6-17. Perceived Level (PL) levels across the linear microphone array for Boom 4.

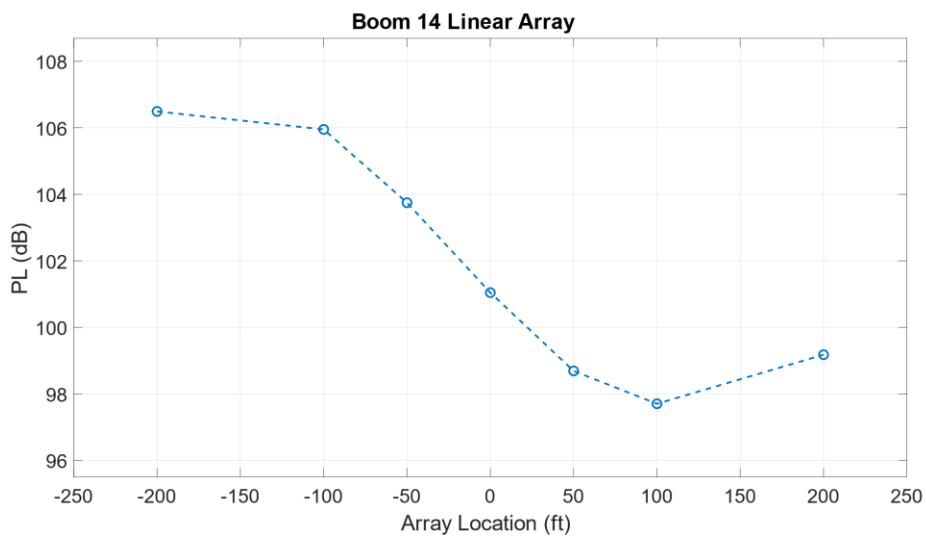

Figure 6-18. Perceived Level (PL) levels across the linear microphone array for Boom 14.

Further investigation into this linear array could provide more detailed estimations of statistical uncertainty in data. Additionally, these observations demonstrate the need for uncertainty quantification in sonic boom measurements. In future testing, using a similar local array could provide models to predict the measurement uncertainty of an array-based measurement similar to CarpetDIEM.

6.5. Additional Observations and Lessons Learned

The CarpetDIEM flight test series was largely successful for BYU and for the larger team. The rapidly-deployable, field-configurable and high-fidelity capability of the PUMA/COUGAR system proved to be an effective combination for sonic boom array measurement. The different triggering methods used by PUMA were all tested at CarpetDIEM, and all proved to be a reliable method of triggering both under supervision and autonomously.

Correlation before the test provided important information that helped lead to a smoother field experience, however, many unforeseen or unmentioned issues surfaced in the field. Transportation proved to be one of the more difficult logistical challenges in the series. Before arrival in the field, all briefings indicated terrain traversable by common road vehicles such as SUVs. However, in practice, it was found that much of the terrain BYU was responsible for staffing contained roads that were difficult to traverse, even with four-wheel drive pickup trucks (many pickup trucks used were too heavy, did not have enough clearance, and lacked off-road tires, which contributed to them struggling on challenging terrain). High-clearance vehicles such as off-road designed sport utility vehicles with four-wheel drive or midsize four-wheel drive trucks equipped with off-road tires would be optimal. Throughout the test campaign as the roads were trafficked more and more, the road conditions further deteriorated until sections of road became nearly impassable.

Communication also proved to be a challenge. Both cellular networks and LMR (Land Mobile Radio) systems did not provide adequate communication links at every point along the array. Better communication systems in future testing would provide a logistical improvement.

7. Future R&D

This R&D program has resulted in the development of an improved weather-robust solution for ground-based acoustical measurements of sonic booms, as well as insights into the broader data acquisition challenge and a method for low-frequency bandwidth enhancement. As part of system testing, BYU participated significantly in both major sonic boom measurement campaigns during the period of performance: QSF18 and CarpetDIEM. Future work could involve detailed wind-tunnel and flow measurements to improve understanding of the mechanisms for the improved wind noise reduction by COUGAR relative to commercial windscreens of similar thickness and the additional improvement offered by COUGARxt relative to COUGAR. This may lead to further design optimizations for measurement performance.

The QSF18 and CarpetDIEM datasets can be leveraged to prepare for eventual X-59 measurements and community testing. The CarpetDIEM measurement site was the planned site for X-59 tests and much can be learned from the data characteristics over the measurement array, including data variability due to changes in meteorology and terrain. Analyses of the BYU and NASA data from QSF18 can also be studied in order to learn about sonic boom characteristics in urban environments, where future X-59 community tests may occur. The ultimate objective is to quantify uncertainty in high-fidelity sonic boom measurements, which is an effort needed to quantify community noise exposure and associated variability during X-59 testing and to develop robust measurement procedures for certifying quiet supersonic civil aircraft.

References

[i] See "ACRP 02-81, Commercial Space Operations Noise and Sonic Boom Measurements," https://apps.trb.org/cmsfeed/TRBNetProjectDisplay.asp?ProjectID=4239

[ii] W. L. Willshire and P. A. Nystrom, "Investigation of Effects of Microphone Position and Orientation on Near-Ground Noise Measurements," NASA Technical Paper 2004, April 1982.

[iii] Federal Aviation Administration, FAR Part 36, Appendix G, "Takeoff Noise Requirements for Propeller-Driven Small Airplane and Propeller-Driven, Commuter Category Airplane Certification Tests on or After December 22, 1988."

[iv] B. Cook, C M. Hobbs, J. Page, and J. Salamone, "Objective data collection and analysis for the waveform and sonic boom perception and response program (WSPR)," Proc. Mtgs. Acoust. **19**, 040153 (2013); doi: 10.1121/1.4799426

[v] J. A. Page, K. K. Hodgdon, P. Krecker, R. Cowert, C. Hobbs, C. Wilmer, C. Koening, T. Holmes, T. Gaugler, D. L. Shumway, J. L. Rosenberger, D. Philips, "Waveforms and Sonic Boom Perception and Response (WSPR): Low-Boom Community Response Program Pilot Test Design, Execution, and Analysis," NASA/CR–2014-218180.

[vi] J. Rathsam and L. J. Cliatt, "Overview of Quiet Supersonic Flights 2018 (QSF18) in Galveston, Texas," J. Acoust. Soc. Am. **146**, 2752 (2019); https://doi.org/10.1121/1.5136527

[vii] G. P. van den Berg, "Wind-induced noise in a screened microphone," J. Acoust. Soc. Am. **119**, 824 (2006); doi: 10.1121/1.2146085

[viii] L. Wang, A.C. Zander, and V.V. Lenchine, "Measurement of the self-noise of microphone wind shields," 18th Australasian Fluid Mechanics Conference, Dec. 2012.

[ix] F. Niu, S. Zhao, X. Qiu, and D. Zhang, "A note on wind velocity and pressure spectra inside compact spherical porous microphone windscreens," J. Acoust. Soc. Am. **147**, EL43 (2020); doi: 10.1121/10.0000592

[x] T. B. Gabrielson and T. M. Marston, "Extraction of infrasonic waveforms from conventional condenser microphones," J. Acoust. Soc. Am. **122**, 2958 (2007); https://doi.org/10.1121/1.2942542

[xi] W. J. Doebler and V. W. Sparrow, "Stability of sonic boom metrics regarding signature distortions from atmospheric turbulence," J. Acoust. Soc. Am. **141**, EL592 (2017); https://doi.org/10.1121/1.4986209

[xii] T. A. Stout and V. W. Sparrow, "Three-dimensional simulation of shaped sonic boom signature loudness variations due to atmospheric turbulence," AIAA paper 2019-2562.

[xiii] V. W. Sparrow, T. A. Stout, K. A. Bradley, and C. M. Hobbs, "SonicBAT: Some highlights and subsequent developments," Proc. ICA 2019, Aachen, Germany.

REPORT DOCUMENTATION PAGE

Form Approved
OMB No. 0704-0188

1. REPORT DATE *(DD-MM-YYYY)*
1-07-2020

2. REPORT TYPE
Contractor Report

3. DATES COVERED *(From - To)*

4. TITLE AND SUBTITLE
Development of a Weather-Robust Ground-Based System for Sonic Boom Measurements

5a. CONTRACT NUMBER
80LARC17C0004

5b. GRANT NUMBER

5c. PROGRAM ELEMENT NUMBER

5d. PROJECT NUMBER

5e. TASK NUMBER

5f. WORK UNIT NUMBER

6. AUTHOR(S)
Kent L. Gee, Daniel J. Novakovich, Logan T. Mathews, Mark C. Anderson, Reese D. Rasband

7. PERFORMING ORGANIZATION NAME(S) AND ADDRESS(ES)
NASA Langley Research Center
Hampton, VA 23681-2199

8. PERFORMING ORGANIZATION REPORT NUMBER

9. SPONSORING/MONITORING AGENCY NAME(S) AND ADDRESS(ES)
National Aeronautics and Space Administration
Washington, DC 20546-0001

10. SPONSOR/MONITOR'S ACRONYM(S)
NASA

11. SPONSOR/MONITOR'S REPORT NUMBER(S)
NASA-CR-2020-5001870

12. DISTRIBUTION/AVAILABILITY STATEMENT
Unclassified
Subject Category-
Availability: NASA STI Program (757) 864-9658

13. SUPPLEMENTARY NOTES
Langley Technical Monitor: Alexandra Loubeau

14. ABSTRACT
This report describes Brigham Young University's (BYU) development and testing of a weather-robust, ground-based system for sonic boom measurements, carried out in support of NASA's Quiet Supersonic Flight (QSF) initiative. The microphone configuration system, referred to as the Compact Outdoor Unit for Ground-based Acoustical Recordings (COUGAR, for the BYU mascot), was tested at NASA's 2018 Quiet Supersonic Flight (QSF18) campaign and at the subsequent 2019 Carpet Determination in Entirety Measurements (CarpetDIEM) program.

15. SUBJECT TERMS
Acoustic; Sonic boom; Supersonic; Microphone

16. SECURITY CLASSIFICATION OF:			17. LIMITATION OF ABSTRACT	18. NUMBER OF PAGES	19a. NAME OF RESPONSIBLE PERSON
a. REPORT	b. ABSTRACT	c. THIS PAGE			STI Help Desk (email: help@sti.nasa.gov)
U	U	U	UU	74	19b. TELEPHONE NUMBER *(Include area code)* (757) 864-9658